# Appendix:
# Supplemental Material

## for "Improved Late Cretaceous and early Cenozoic Paleomagnetic Apparent Polar Wander Path for the Pacific Plate" by Beaman, Sager, Acton, Lanci, and Pares

The data set used for this study is large and contains some newly measured data, some unpublished data and some previously- published data that have been altered or reanalyzed. Space limitations do not allow us to describe these data in the main body of the article, so details are provided here. This appendix contains additional sediment and basalt core data from DSDP Site 577 and ODP Sites 869, 883, 884, 887, 1218, 1219, 1220, and 1224.

## NEW DATA

### Sites 884 and 869

Our paleocolatitude data set includes new inclination measurements made from sedimentary core samples from two ODP sites (869, 884) that had not been previously subjected to paleomagnetic analysis for the early Cenozoic. Discrete sample paleomagnetic measurements were made on samples taken from the working halves of the ODP cores from Site 869, Hole A (869A) and Site 884, Hole B (884B) (Table A1, A2). We combine the description of these two sets of cores in this section because they were measured together.

Oligocene and Eocene sections of cores from Holes 884B and 869A are composed of both hard and soft sedimentary rock facies such as nannofossil chalks and oozes, respectively. We sampled five hydraulic piston cores (APCs) from Hole 869A, taking two to three discrete samples from each core section (1.5 m-length), depending

upon the amount of intact core material. A total of 101 samples were taken from cores 143-869A-5H through 143-869A-9H. From Hole 884B, we sampled expanded core barrel (XCB) cores 145-884B-70X through 145-884B-87X, with approximately two samples coming from each core, for a total of 205 samples. The softer, less consolidated samples of Hole 869A were extracted using clear plastic sampling cubes. The harder, more consolidated chalks and claystones of Hole 884B were sampled using a metal, mini-push coring device with the samples placed into plastic cubes.

***Methods***

The core samples from holes 869A and 884B underwent natural remnant magnetization (NRM) analysis in the paleomagnetism laboratory at the University of California- Davis campus. In the lab, the samples were subjected to alternating field demagnetization (AFD) to remove secondary magnetization overprinting the primary magnetization (ChRM) gained at deposition. AFD was performed with a 2G Enterprises 755-1.65UC DC SQUID Superconducting (u-channel) Rock Magnetometer fitted with a discrete sample tray and interfaced with a PC for automated data acquisition [http://paleomag.geology.ucdavis.edu/instruments.htm]. Samples showing irregular results on the u-channel magnetometer due to low magnetic moment values were also run on an 2G Enterprises 760-3.0 AC SQUID Superconducting Rock Magnetometer (discrete sample cryogenic magnetometer). The discrete cryogenic magnetometer is more sensitive, but also more time consuming than the u-channel magnetometer, so only low intensity samples were run on the former. The AFD was initially carried out on a few samples from each site in steps of 5 and 10 milliteslas (mT), with increasing field

strength from 0 to 80 mT, to determine which steps were best at removing the magnetic overprint and maintaining the consistency of the resulting inclination values. Because the magnetizations were weak and results noisy for high demagnetizing fields, we only demagnetized most samples from Hole 884B up to 50 mT and samples from Hole 869A up to 35 mT.

AFD data from Holes 869A and 884B were analyzed using principal component analysis (PCA) to determine the ChRM direction [Kirschvink, 1980]. For most samples, we used a PCA solution that was not anchored to the origin, but on some weakly magnetic samples or those that had few consistent demagnetization steps, we used an anchored solution (Figures A1, A2). Stable inclination and declination values from the PCA analysis were used to establish polarity zones in the cores. These zones were compared to the ODP biostratigraphy [Firth, 1995; Barron et al., 1995] to determine a magnetostratigraphy and corresponding age range for the sediments in each core. The inclination data from the PCA analysis were also used to calculate mean paleocolatitudes for the sediment cores [Cox and Gordon, 1984].

A subset of the Hole 884B samples was analyzed for anisotropy of magnetic susceptibility (AMS) to look for evidence that inclination shallowing influenced the ChRM directions. The AMS analysis was performed at UC Davis on a KappaBridge KLY-2 Susceptibility Meter using the standard fifteen position/3 axis sample analysis [Jelínek, 1977]. The degree of AMS is important because it relates to inclination error [Kodama and Sun, 1992] and by measuring the AMS, the level of error in the inclination measurements can be evaluated [Blow and Hamilton, 1978; Deamer and Kodama, 1990;

Kodama and Sun, 1992; Hodych et al., 1999]. Hole 869A samples did not undergo AMS analysis because they are weakly magnetic and were deposited close to the equator, where they should not be significantly affected by inclination shallowing.

This subset of samples from Hole 884B were also evaluated for inclination shallowing by measuring the anisotropy of anhysteretic remanent magnetization (AARM) present. AARM was measured on the 2G Enterprises u-channel magnetometer at UC Davis. AARM analysis was performed using the Hodych et al. [1999] method, which uses a linear regression to evaluate values of the tangent of inclination [tan I] compared to $ARM_{min}/ARM_{max}$ and $K_{min}/K_{max}$ values. If consistent inclination shallowing is present, there should be a linear correlation between tan I and $ARM_{min}/ARM_{max}$. This correlation can be used to predict the inclination of the sediments prior to the shallowing, and thus estimate the amount of shallowing present [Hodych et al. 1999; Mendenhall and Sincich, 1993]. An examination of the types of magnetic carriers present in the sediments from Holes 884B and 869A was also performed using hysteresis loop analyses on a few representative samples from each hole. This hysteresis analysis was performed on the UC Davis Princeton MicroMag 2900 Alternating Gradient Magnetometer (MicroMag). Small subsamples, < 50 milligrams in size, were removed from the selected paleomagnetic sample cubes after the cubes underwent AFD. The MicroMag allowed measurements of sample bulk coercive force ($H_c$), as well as values of remanent ($M_r$) and saturation ($M_s$) magnetization.

A few samples from Hole 869A had magnetic intensities too weak to be measured on the MicroMag. These weak samples were instead evaluated by inducing a

progressive isothermal remanent magnetization (IRM) on the samples using a pulse magnetizer. Induced fields were increased to give an IRM acquisition curve, which gives a indication of magnetic carrier coercivity [Dunlop, 1972]. The saturating magnetic (IRM) pulse was applied to the samples using the u-channel magnetometer and increased in steps from 0 to 1000 mT. IRM acquisition curves and hysteresis loop plots were compared with plots of known ferromagnetic minerals to determine the primary magnetic carriers in our samples [Dunlop, 1972; Day et al., 1977].

***Results***

Hole 869A

*Rock Magnetism*

Hysteresis was performed on one sample from Hole 869A with the result suggesting pseudo-single domain magnetite as the magnetic carrier. Thirty-five other samples underwent SIRM analysis because the weak magnetization of the sediments made hysteresis analysis difficult. The SIRM analysis of the samples exhibited rapid magnetization saturation (Fig. A3). This rapid saturation of the magnetic grains is characteristic of titanomagnetite, so this test also implies magnetite as the predominate magnetic carrier in the sediment of Hole 869A [Dunlop, 1972; Day et al, 1977].

*Magnetostratigraphy*

For determination of magnetostratigraphy, we were unable to use inclinations to determine polarity because the sediments were deposited near the equator. Instead, we used declination reversals (flips of ~180°) to establish changes in the samples' magnetic polarity. However, before using the declination measurements, the sample

magnetizations had to be azimuthally oriented. Core declination corrections were determined onboard during Leg 143 coring operations by the Shipboard Scientific Party [1993a] using the multishot tensor tool camera [Fisher et al., 1993]. The corrected declinations and observed polarity chronozones were consistent with biostratigraphic zonations assigned to the core sections 143-869A-5H-1 through 143-869A-9H-7 by Firth [1995], which were matched to the geologic time scale (Fig. A4) [Gradstein et al., 2004].

*Average Paleocolatitude*

Analysis of the demagnetization results of samples from Hole 869A resulted in forty-four inclination measurements suitable for calculating a mean paleocolatitude for the Early Oligocene [Kirschvink, 1980; Cox and Gordon, 1984]. The calculated paleocolatitude from Hole 869A is 85.4° ± 3.9° (standard error; N=44) [Cox and Gordon, 1984]. The paleocolatitude has an average age of 32.5 ± 2.5 Ma (standard deviation; Table 1). The age was determined from correlation of the magnetostratigraphy and biostratigraphy (Table A1; Fig. A4) [Shipboard Scientific Party, 1993a; Firth, 1995; Gradstein et al., 2004].

Hole 884B

*Rock Magnetism*

Hysteresis analysis on twenty samples from Hole 884B characterized the primary magnetic remanence carrier for these sediments as pseudo-single domain magnetite (Fig. A5; Table A3).

*Magnetostratigraphy*

Correlation of the biostratigraphy and magnetostratigraphy from the demagnetized samples for Hole 884B was more complex than that for Hole 869A. This complexity was due to a slight disagreement between the biostratigraphy and the magnetic polarity of the Hole 884B discrete sediment samples taken from core sections 145-884B-71X-5 to 145-884B-72X-6 (~660 to 670 mbsf).

The biostratigraphy in the upper measured section of Hole 884B showed that the last occurrence of (LO) of the calcareous nannofossil *Reticulofenestra bisecta* of pelagic zonation NP 25 occured between 145-884B-70X-1, 0 cm and 145-884B-70X-1, 48 cm, giving this interval an age of 23.1 to 27.1 Ma [Barron et al., 1995; Gradstein et al., 2004]. The discrete samples from this section displayed reversed magnetic polarity, and matching the polarity with the biostratigraphy, this section was assigned to Chron 8r (26.18 to 26.71 Ma). The biostratigraphy also gave the first occurrence (FO) of diatom *Rocella vigilans* and LO of calcareous nannofossil *Reticulofenestra umbilica* between sections 145-884B-70X-CC and 145-884B-71X-CC, making core section 145-884B-71X-7 up to 32.4 Ma in age [Shipboard Scientific Party, 1993c; Pak and Miller, 1995; Gradstein et al., 2004]. Thus, first and last occurrences in the biostratigraphy from cores 145-884B-70X to 145-884B-71X implied a minimum age interval of 26.7 Ma to 32.4 Ma, ~6 Myr.

The discrete samples from this section included both normal and reversed polarities, with several reversals observed downcore (Fig. A6). However, there were not enough recorded reversals for the magnetostratigraphy of core sections 145-884B-71X-1

through 145-884B-72X-6 to match the assigned biostratigraphic age range. The GPTS [Gradstein et al., 2004; Cande and Kent, 1995] for this time interval shows 11 reversals (chrons 9n to 12r) whereas only 7 reversals are recorded in this interval from Hole 884B. The missing polarity zones support the existence of an unconformity, but of uncertain duration. Changes in the lithology of the core sections also suggested the presence of an unconformity in the lowermost part of core 145-884B-71X; however, the exact timing and duration of the unconformity were not determined. Changes in sedimentation rates could have also occurred during this time, further complicating the magnetostratigraphy. Because of this uncertainty, we show two alternative interpretations of polarity chrons in this section of Figure A6. Nonetheless, the difference in implied age is small and does not substantially affect our paleomagnetic pole calculations, which used interpretation 1, shown in Figure A6.

The Eocene-Oligocene boundary was observed in the sediments just below a zone of shallow inclination, and uncertain polarity. Even though the polarity above this uncertain zone was normal, polarity chron assignments in much of sections 145-884B-75X-5 to 145-884B-82X-4 were unclear because the inclinations were variable. These core sections also showed signs of slumping and re-deposition, making conclusive polarity and age assignments problematic.

The older core sections (145-884B-83X-3 to 145-884B-87X-6) give a clear polarity chron record that is consistent with the biostratigraphy. These core sections were assigned to chrons C19r through C22n, 40.7 to 49.4 Ma (Fig. A6).

*Average Paleocolatitude*

Hole 884B produced three useable paleocolatitude values; one for the Oligocene and two for the Eocene (Table 1). Forty-nine samples were averaged to calculate the Oligocene paleocolatitude of 48.8° ± 9.3° (N=49) with an age of 30.0 Ma. The Eocene paleocolatitudes calculated for Hole 884B are 64.5° ± 6.3° for 41.2 ± 0.5 Ma (N =11) and 49.7°± 7.5° for 45.7 ± 2.9 Ma (N=26).

*Inclination Shallowing Study*

The discrete paleomagnetic samples from Hole 884B measured for AMS produced corrected anisotropy degree (P`) values between 1.00 and 1.09. All but two of the samples from Hole 884B had values of P`≤ 1.05, and thus are considered weakly anisotropic [Hrouda, 1982; Weaver et al., 2004]. The two samples with larger P` (>1.05) values were classified as weakly to moderately anisotropic (Table A4).

Because the AMS results from Hole 884B showed that the sediments were weakly anisotropic, we used the method of Hodych et al. [1999] to attempt to quantify the inclination shallowing. Using the method of Hodych et al. [1999] and Mendenhall and Sincich [1993], the tan I versus $ARM_{min}/ARM_{max}$ correlation yielded a predicted inclination of 56.0° +8°/-12.8° (95% confidence) for Hole 884B sediments and the tan I versus $K_{min}/K_{max}$ analysis indicated an inclination of 57.2° +6.9°/-12.0° (95% confidence) (Fig. A7; Tables A4, A5). Both of these results are higher than the calculated 50.2° ± 12.8° (95% confidence) mean inclination of the discrete samples, suggesting that the sediment may have been affected by inclination shallowing. However, the uncorrected mean inclination is within the 95% confidence limits of the

corrected site inclination, suggesting that the inclination shallowing may not be significant. The large confidence limits of the predicted (pre-shallowing) inclination are probably due to the scatter of inclinations. This data set also produced a low regression coefficient value (R = 0.12), suggesting a poor correlation of the inclination values and further implying that the inclination shallowing correction is insignificant. The predicted 6° correction for inclination shallowing is slightly more than the expected difference of 2° predicted by our empirical analysis of paleocolatitudes, but the confidence limits on the correction are large enough that the two are not significantly different (see Discussion).

**Site 883**

Some sections of the sediment cores from ODP Leg 145 Site 883, Hole B contained sediments of Eocene age appropriate for inclusion in our study. Forty-one discrete samples from the working halves of core sections 145-883B-76X -1 to 145-883B-85X-3 were used to calculate two mean paleocolatitude values for the Eocene.

***Methods***

Samples were collected from Hole 883B cores using plastic sample cubes. Measurements were made on the Texas A&M University CTF discrete sample cryogenic magnetometer. The samples from Hole 883B were AF demagnetized in 5 to 10 mT steps up to 80 mT using a Schoenstedt GSD-1 demagnetizer. These measurements were used for principle component analysis (PCA) to establish stable ChRM inclination values (Fig. A8; Table A6). We used the biostratigraphy of Barron et al. [1995] and the Gradstein et al. [2004] time scale to assign an age to the sediment samples of early and

mid to late Eocene. Because we measured so few samples from this hole, we did not attempt to modify the magnetostratigraphy from the initial analysis of the hole on ODP Leg 145 [Shipboard Scientific Party, 1993b].

***Results***

The 883B samples produced two mean paleocolatitudes [Cox and Gordon, 1984] for late and early Eocene data groups (Table A6). The paleocolatitude calculated for the early Eocene is 61.5°± 8.1° (N=29) with an average age of 52.5 ± 3.5 Ma. The late Eocene average paleocolatitude is 53.9 ± 9.2° (N=12) and has an average age of 41.8 ± 5.3 Ma (Table 1) [Barron et al., 1995; Gradstein et al., 2004].

**Site 887**

ODP Leg 145 cored 83.7 M into igneous basement atop Patton-Murray Seamount recovering 16.4 m of basalt flows [Shipboard Scientific Party, 1993d]. The recovered units were subdivided into five flow units based on chilled and glassy margins, the uppermost being a massive sill and the rest, lava flows [Shipboard Scientific Party, 1993d]. $^{40}Ar/^{39}Ar$ geochronology studies yielded an age of 17 Ma for the sill and 27.4 ± 0.4 Ma for one of the flows [Keller et al., 1995].

***Methods***

We obtained 31 2.5 cm (1 in.) diameter mini-cores from the 887D igneous core working halves for paleomagnetic analysis. Samples were measured with a CTF discrete samples cryogenic magnetometer at Texas A&M University. All samples were subjected to AF demagnetization at 5 mT steps up to 50 mT and 10 mT steps to 80 mT.

Demagnetization data were examined on Zijderveld plots and ChRM inclinations were calculated using PCA.

***Results***

Samples were well behaved and routinely gave simple demagnetization plots with linear decay to the origin of the Zijderveld plot.

Inclinations from the lower four igneous units were used to calculate a mean inclination. Data from the upper unit was not used because of its young age. Samples from units 2-4 gave indistinguishable inclination groups and were combined, thus the Holes 887D paleocolatitude is based on only 2 independent units (N=2) (Fig. A9; Table A7). The mean calculated paleocoaltitude is 56.2° ± 7.5°, using the Cox and Gordon [1984] method.

**Site 1224**

Six holes were cored at Site 1224 (27° 53.363'N, 141° 58.758'W) during ODP Leg 200, with the deepest hole (1224F) penetrating 146.5 m into a 46-Ma section of normal oceanic crust [Shipboard Scientific Party, 2003].

***Methods***

At least 14 cooling or flow units were recovered, which were subdivided into three main stratigraphic or morphological units during Leg 200: Unit 1 (28.0-62.7 mbsf; 0-34.7 msb) contains two massive basalt flows, Unit 2 (62.7-133.5 mbsf; 34.7-105.5 msb) contains thin flows and pillows, and Unit 3 (133.5-161.8 mbsf; 105.5-133.8 msb) contains basalt flows of intermediate thickness alternating with thin flows and pillows [Shipboard Scientific Party, 2003]. The cooling unit contacts are based mainly on the

occurrence of glassy intervals observed in the recovered cores. The true number of cooling units is likely somewhat larger than the described 14 units because some contact zones and complete flow units were likely not recovered.

Measurements were made using the cryogenic magnetometers (2G Enterprises model 760-3.1 LC) onboard the *JOIDES Resolution* [Shipboard Scientific Party, 2003] and using the cryogenic (2G Enterprises model 760-1.65 UC) and spinner (AGICO model JR5) magnetometers in the paleomagnetism laboratory at the University of Hawaii. Discrete samples (~8 $cm^3$ and ~1 $cm^3$ cubes) were typically AF demagnetized up to 80 mT in steps of 1-5 mT. Thermal demagnetization was conducted in 20°-60°C steps from 80°C to 620°C. Mean directions for the discrete samples were determined by PCA.

***Results***

Paleomagnetic results were obtained for 204 discrete samples (Table A8). All samples have a drilling overprint characterized by a low-coercivity component that is steep (up or down) and has a radial-horizontal component directed toward the center of the core (Fig. A10). For most samples, ~10-mT AF demagnetization or 380°C thermal demagnetization generally removed the drilling overprint, except for those samples taken from near the periphery of the core. For these samples, the overprint could not be fully removed by AF or thermal demagnetization as it completely overlaps the coercivity and unblocking spectra of the ChRM [e.g., Fig. F62 in Shipboard Scientific Party, 2003].

In some more highly altered intervals from Cores 1224F-6R through 12R, a normal polarity overprint can be separated from the drilling overprint owing to the high

coercivity of the former. The inclination of this component, which is about 15-30°, is shallower than expected for a Brunhes overprint, so we suspect it was acquired within a normal polarity interval shortly after Chron C20R time (43.789-46.264 Ma). If this overprint was caused by alteration, it indicates that alteration was occurring more than 2 m.y. after the extrusion of the basalts (after the end of Chron 20R). Alternatively, the composition of the titanomagnetite and titanomaghemite in some samples may be such that self reversal occurs upon cooling of the flow immediately after extrusion [e.g., Krasa, 2003], in which case the low inclination normal overprint is merely a mirror image of the primary magnetization.

Rock magnetic results from hysteresis analyses and from temperature vs. susceptibility measurements indicate the remanence is carried by PSD titanomagnetite and titanomaghemite. Overall, the basalt flows at Site 1224 display paleomagnetic and rock magnetic properties common to ocean basalts.

Of the 204 samples, 126 samples gave stable ChRM directions, based on assessment of orthogonal vector plots and principal component analysis (Table A8). We rejected 46 samples because the ChRM could not be isolated from the drilling overprint or from the normal polarity overprint of unknown origin. We did not use 28 other samples because they were duplicate samples (specimens) from intervals where multiple samples were taken to study the drilling overprint. We also rejected 4 other samples because they gave magnetization directions that appeared to be either outliers or were from units that had distinct directions but that gave too few results (<4) to be considered independent samples of the geomagnetic field (i.e., a secular variation units).

The results were grouped into secular variation (SV) units based on the location of directional changes and flow unit contacts or coring gaps where flow unit contacts could have existed but were not recovered. Because the cores are azimuthally unoriented, only the inclination is used for determining a change in the paleomagnetic direction.

We have grouped the directions conservatively in to five SV units (Fig. A11). The mean inclination is determined for each SV unit (Table A9) and then the overall mean inclination and paleolatitude is estimated from these SV unit means. For comparison and completeness, we compute the means using both the method of Cox and Gordon [1984], which give a paleocolatitude of 83.0° ± 8.2° (N=5), and that of McFadden and Reid [1982], which gives a paleocolatitude of 83.1° ± 11.9°. For consistency with the other paleocolatitude data, the Cox and Gordon error estimate was used in the pole calculations (Table 1).

The average age of the Site 1224 paleocolatitude is 46.2 ± 0.4 Ma based on the weighted average of three $^{40}Ar/^{39}Ar$ plateau dates [Acton and Duncan, in prep.]. This age is consistent with the position of Site 1224 within Anomaly 20R and very near the Anomaly 21N/20R boundary.

## REANALYZED DATA

### Site 577

Sediment paleocolatitudes for Holes 577 and 577A of DSDP Site 577 were recalculated from the stable inclination data of Bleil [1985]. The original

paleocolatitudes were calculated over large time spans and we wanted to limit the ages of the paleocolatitudes to a few million years at most. The inclination data were assigned revised ages using the time scale of Gradstein et al. [2004], and grouped by polarity chrons. The method of Cox and Gordon [1984] was used to calculate mean paleocolatitudes. Fourteen paleocolatitudes were calculated from Hole 577 and 577A cores. (Table 1; main article).

**Sites 1218 and 1219**

U-channel stable inclination data published as magnetostratigraphies for Sites 1218 and 1219 in Lanci et al. [2005] were converted into paleocolatitudes and averaged using the Cox and Gordon [1984] method. Site 1218 and 1219 magnetostratigraphic age data from Lanci et al. [2005] were adjusted to the Gradstein et al. [2004] time scale. In total, we used 2507 measurements for Site 1218 and 1652 measurements for Site 1219. The large number of measurements was a result of closely-spaced u-channel inclination measurements.

With the large amount of data, we could have calculated individual paleocolatitudes for each polarity chron in the measured section (almost two dozen total) however, with so many paleocolatitudes, each with compact uncertainty, these data would have assumed undue weight in determining the mean pole location. Thus, we simply averaged these data into paleocolatitudes for the early and late Oligocene. Because different chrons contributed different numbers of data, mean colatitude ages were computed by weighing each chron by the number of samples from that chron. This

data weighting is the cause of the uneven age uncertainties for the Site 1218 and 1219 mean paleocolatitudes.

Two mean paleocolatitudes were calculated for Site 1218 and one for Site 1219 (Table 1; main article). One of the Site 1218 paleocolatitudes is 87.5° ± 2.7° and has an average age of 26.3 +2.0/-3.2 Ma, calculated from N=1668 inclination measurements. The second Site 1218 paleocolatitude, 87.4° ± 3.7°, has an average age of 29.2 +0.8/-0.7, determined from N=839 measurements. Site 1219 has a paleocolatitude value of 92.9° ± 3.1° with an age of 32.0 +2.0/-1.6 Ma, from N=1652 measurements.

**Site 1220**

Stable inclination data published in the magnetostratigraphy of Parés and Lanci [2004] for Site 1220 were used to calculate two Eocene paleocolatitudes. These paleocolatitudes were calculated using the method of Cox and Gordon [1984] and assigned ages from the Gradstein et al. [2004] time scale. The first paleocolatitude, representing mid Eocene chron C20n, was calculated from N=772 inclinations, resulting in a colatitude value of 94.5° ± 3.8°, and an age 42.2 ± 0.6 Ma. The second Site 1220 paleocolatitude of 92.4° ± 2.8° was calculated from N=161 inclinations. It represents mid-Eocene chron C20r with an age of 44.1 ± 1.3 Ma.

**Age Calculations**

Mean ages for the stratigraphic stage poles were determined using data importances assigned by the pole calculating program (Table A10). The mean age of each datum was multiplied by its importance to get a weighted age value. These age values were then totaled and the sum divided by the number of data included in the pole.

This resulted in an average age for each pole that takes into account the influence of each datum age on the mean pole age.

The time window pole ages were determined in a similar manner, however each age datum was included in multiple age calculations due to the overlapping nature of the data in the windowing technique (Table A11). The time window age calculations (Table A11) are provided for the time window APWP (Figure 9; main article).

## REFERENCES

Anson, G.L. and. K. P. Kodama, Compaction-induced inclination shallowing of the post-depositional remanent magnetization in a synthetic sediment, *Geophys. J. R. Astr. Soc.* 88, 673-692, 1987.

Barron, J.A., I.A. Basov, L. Beaufort, G. Dubuisson, A.Y. Gladenkov, J.J. Morley, M. Okada, G. Ólafsson, D.K. Pak, A.P. Roberts, V.V. Shilov, and R.J. Weeks, Biostratographic and magnetostratigraphic summary, *Proc. ODP, Sci. Res., 145,* 559-576, 1995.

Bleil, U., The magnetostratigraphy of northwest Pacific sediments, Deep Sea Drilling Project Leg 86, in *Init. Repts., DSDP 86,* US Govt. Printing Office, Washington, DC, 441-458, 1985.

Blow, R.A. and N. Hamilton, Effect of compaction on the acquisition of a detrital remanent magnetization in fine-grained sediments, *Geophys. J. R. Astr. Soc.*, 52, 13-23, 1978.

Cande, S.C. and D.V. Kent, A new geomagnetic polarity time scale for the Late Cretaceous and Cenozoic, *J. Geophys. Res*., 97, 13917-13951, 1995.

Cox, A. and R.G. Gordon, Paleolatitudees determined from paleomagnetic data from vertical cores, *Rev. Geophys. Space Phys.*, 22, 47-72, 1984.

Day, R., M.D. Fuller and V.A. Schmidt, Hysteresis properties of titanomagnetites: Grain size and composition dependence, *Phys. Earth Planet. Int.*, 13, 260-267, 1977.

Deamer G.A. and K.P. Kodama, Compaction induced inclination shallowing in synthetic and natural clay-rich sediments, *J. Geophys. Res*., 95, 4511-4529, 1990.

Dunlop, D.J., Magnetic mineralogy of heated and unheated red sediments by coercivity spectrum analysis, *Geophys. J. R. Astr. Soc.*, 27, 37-55, 1972.

Firth, J.V., Data report: Cenozoic calcareous nannofossils of Hole 869A, equatorial Pacific Ocean, *Proc. ODP, Sci. Res., 143,* 567-570, 1995.

Fisher, A.T., K. Becker, P.D. Rabinowitz, J. Baldauf, and T.J.G. Francis, A guide to ODP tools for downhole measurements, Ocean Drilling Program, Texas A&M University, Technical Note 10, (http:www-odp.tamu.edu/publications/tnotes/tn10/10toc.html), 1993.

Gradstein, F.M., J.G. Ogg, A.G. Smith, F.P. Agterberg, W. Bleeker, R.A. Cooper, V. Davydov, P. Gibbard, L.A. Hinnov, M.R. House, L. Lourens, H.P. Luterbacher,

J. McArthur, M.J. Melchin, L.J. Robb, J. Shergold, M. Villeneuve, B.R. Wardlaw, J. Ali, H. Brinkhuis, F.J. Hilgen, J. Hooker, R.J. Howarth, A.H. Knoll, J. Laskar, S. Monechi, K.A. Plumb, J. Powell, I. Raffi, U. Röhl, P. Sadler, A. Sanfilippo, B. Schmitz, N.J. Shackleton, G.A. Shields, H.Strauss, J. Van Dam, T. van Kolfschoten, J. Veizer, and D. Wilson, *A Geologic Time Scale 2004*, Cambridge University Press, Cambridge, 589 p., 2004.

Hodych, J. P., S. Bijaksana, and R. Pätzold, Using magnetic anisotropy to correct for paleomagnetic inclination shallowing in some magnetite-bearing deep-sea turbidites and limestones, *Tectonophysics*, 307, 191-205, 1999.

Hrouda, F., Magnetic-anisotropy of rocks and its application in geology and geophysics, *Geophysical Surveys* 5 (1), 37-82, 1982.

Jelínek, V., *The Statistical Theory of Measuring Anisotropy of Magnetic Susceptibility of Rocks and its Applications*, 88 pp, Geofysika, Brno, Czechoslovakia, 1977.

Keller, R. A., R. A. Duncan, and M. R. Fisk, Geochemistry and $^{40}Ar/^{39}Ar$ Geochronology of basalts from ODP Leg 145 (north Pacific transect), *Proc. ODP, Sci. Res., 145*, 333-344, 1995.

Kirschvink, J.L., The least squares line and plane and the analysis of paleomagnetic data, *Geophys. J. R. Astr. Soc.* 62 (3), 699-718, 1980.

Kodama, K.P. and W. W. Sun, Magnetic anisotropy as a correction for compaction-caused paleomagnetic inclination shallowing, *Geophys. J. Int.*, 111, 465-469, 1992.

Krasa, D., V.P.Shcherbakov, T. Kunzmann, and N. Petersen, Self-reversal of remanent magnetization in basalts due to partially oxidized titanomagnetites, *Geophys. J. Int.* 162, 115-136, 2005.

Lanci, L., J.M. Parés, J.E.T. Channell, and D.V. Kent, Oligocene magnetostratigraphy from equatorial Pacific sediments (ODP Sites 1218 and 1219, Leg 199), *Earth Planet. Sci. Lett*., 237, 617-634, 2005.

McFadden, P.L., and A. Reid, Analysis of paleomagnetic inclination data, *Geophys. J. R. Astr. Soc.* 69, 307-319, 1982.

Mendenhall, W. and T. Sincich, *A Second Course in Business Statistics: Regression Analysis*, Macmillan, New York, 859p., 1993.

Pak, D.K and K.G. Miller, Isotopic and faunal record of Paleogene deep-water transitions in the north Pacific, in *Proc. ODP, Sci. Res., 145*, 265-281, 1995.

Parés, J. M. and L. Lanci, A Middle Eocene-Early Miocene magnetic polarity stratigraphy in equatorial Pacific sediments (ODP Site 1220), in *Timescales of the Paleomagnetic Field*, edited by *J.E.T. Channell, D.V. Kent, W. Lowrie, and J.G. Meert, Geophys. Mono. 145*, AGU, 131-140, 2004.

Shipboard Scientific Party, Site 869, *Proc. ODP, Init. Repts., 143,* 297-348, 1993a.

Shipboard Scientific Party, Site 883, *Proc. ODP, Init. Repts 145*, 121-208, 1993b.

Shipboard Scientific Party, Site 884, *Proc. ODP, Init. Repts 145*, 209-302, 1993c.

Shipboard Scientific Party, Site 887, *Proc. ODP, Init. Repts 145*, 335-391, 1993d.

Shipboard Scientific Party, Leg 199 summary and Sites 1218, 1219, 1220, *Proc. ODP, Init. Repts.,199,* [CD-ROM], Available from: Ocean Drilling Program, College Station, TX 77845-9547, 2002.

Shipboard Scientific Party, Leg 200 summary and Site 1224, *Proc. ODP, Init. Repts. 200,* [CD-ROM], Available from: Ocean Drilling Program, College Station, TX 77845-9547, 2003.

Weaver, R., A.P. Roberts, R. Flecker, D.I.M. Macdonald, Tertiary geodynamics of Sakhalin (NW Pacific) from anisotropy of magnetic susceptibility fabrics and paleomagnetic data, *Tectonophysics,* 379, 25-42, 2004.

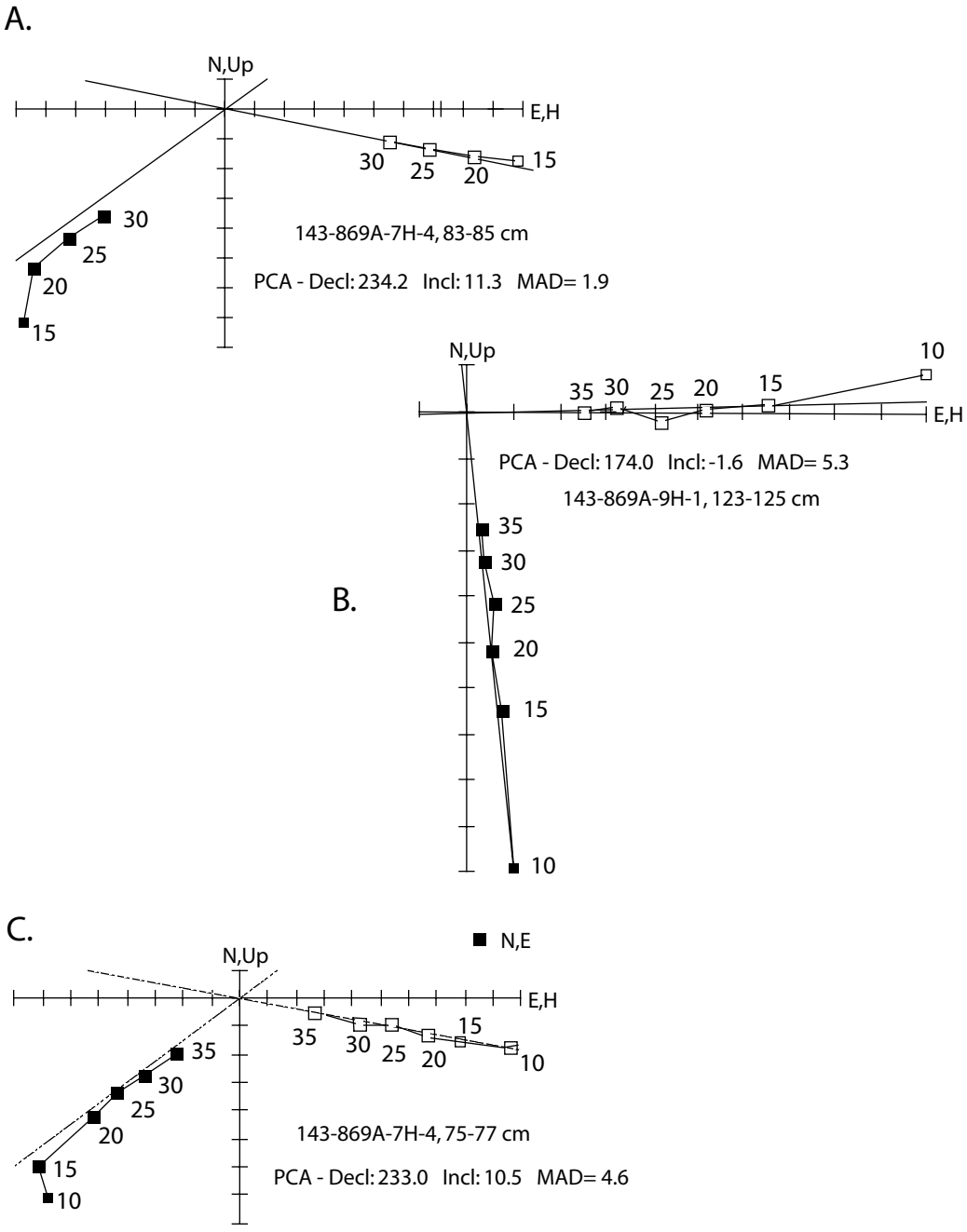


Figure A1. Zijderveld diagrams showing principal component analysis of three Hole 869A samples (unanchored); squares denote AF demagnetization steps in milliteslas (mT); open squares are vertical plane; solid squares are horizontal plane. A) Sample 143-869A-7H-4, 83-85 cm; B) Sample 143-869A-9H-1, 123-125 cm; C) Sample 143-869A-7H-4, 75-77 cm.

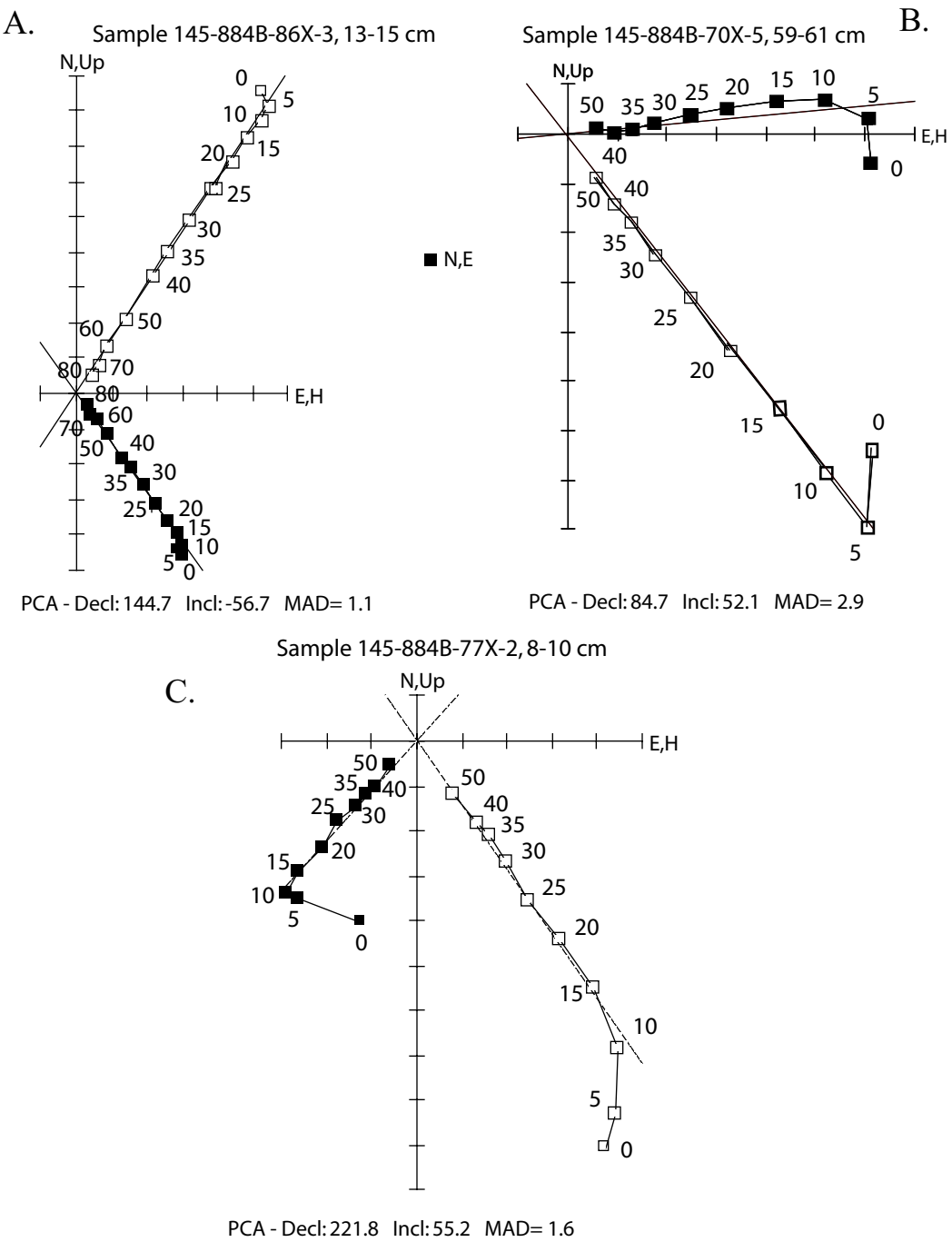


Figure A2. Zijderveld diagrams showing principal component analysis and stable inclinations of three Hole 884B samples (anchored); squares denote AF demagnetization steps in milliteslas (mT); open squares are vertical plane; solid squares are horizontal plane. A) Sample 145-884B-86X-3, 13-15 cm; B) Sample 145-884B-70X-5, 59-61 cm; C) Sample 145-884B-77X-2, 8-10 cm.

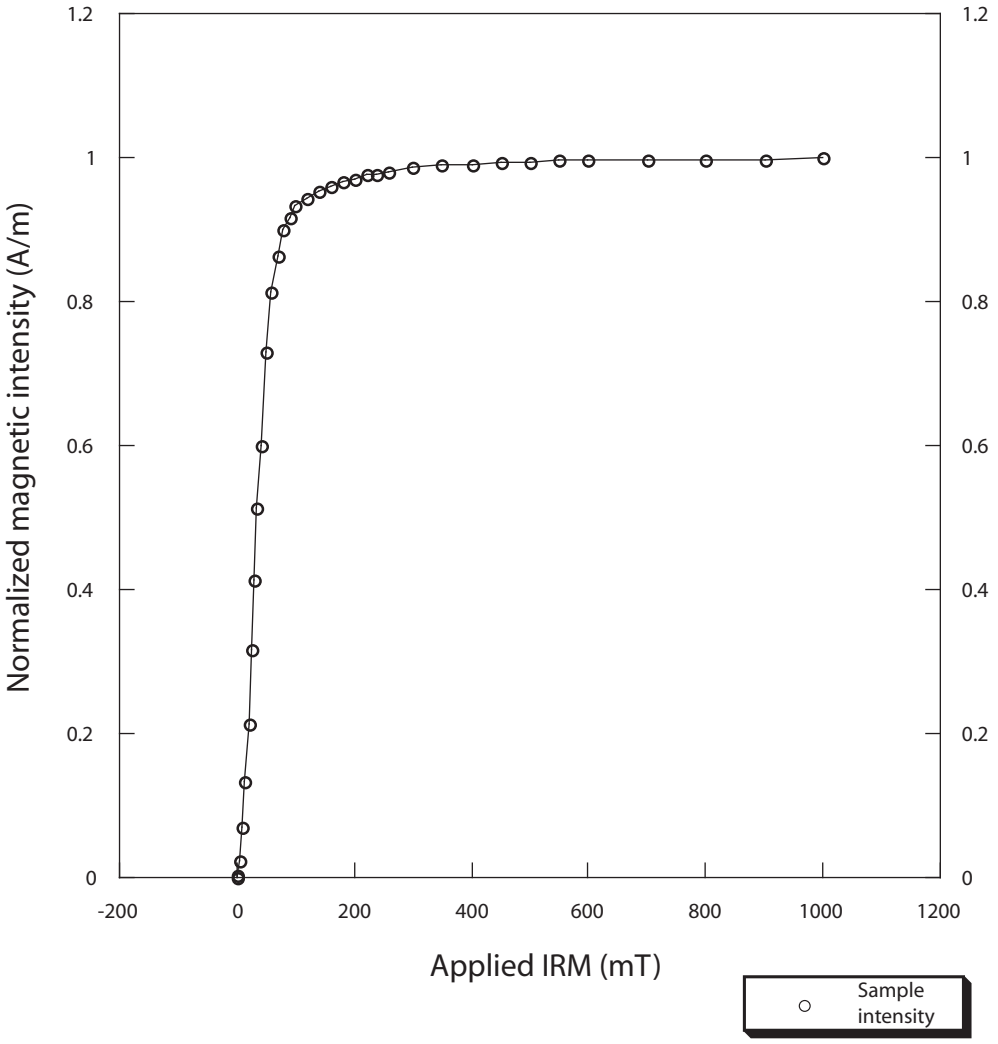


Figure A3. Average (N=35) normalized magnetic intensities of Hole 869A discrete samples when saturated by IRM pulse. Measurements show samples are saturated by 200 mT of applied IRM. Rapid magnetization saturation is characteristic of titanomagnetites.

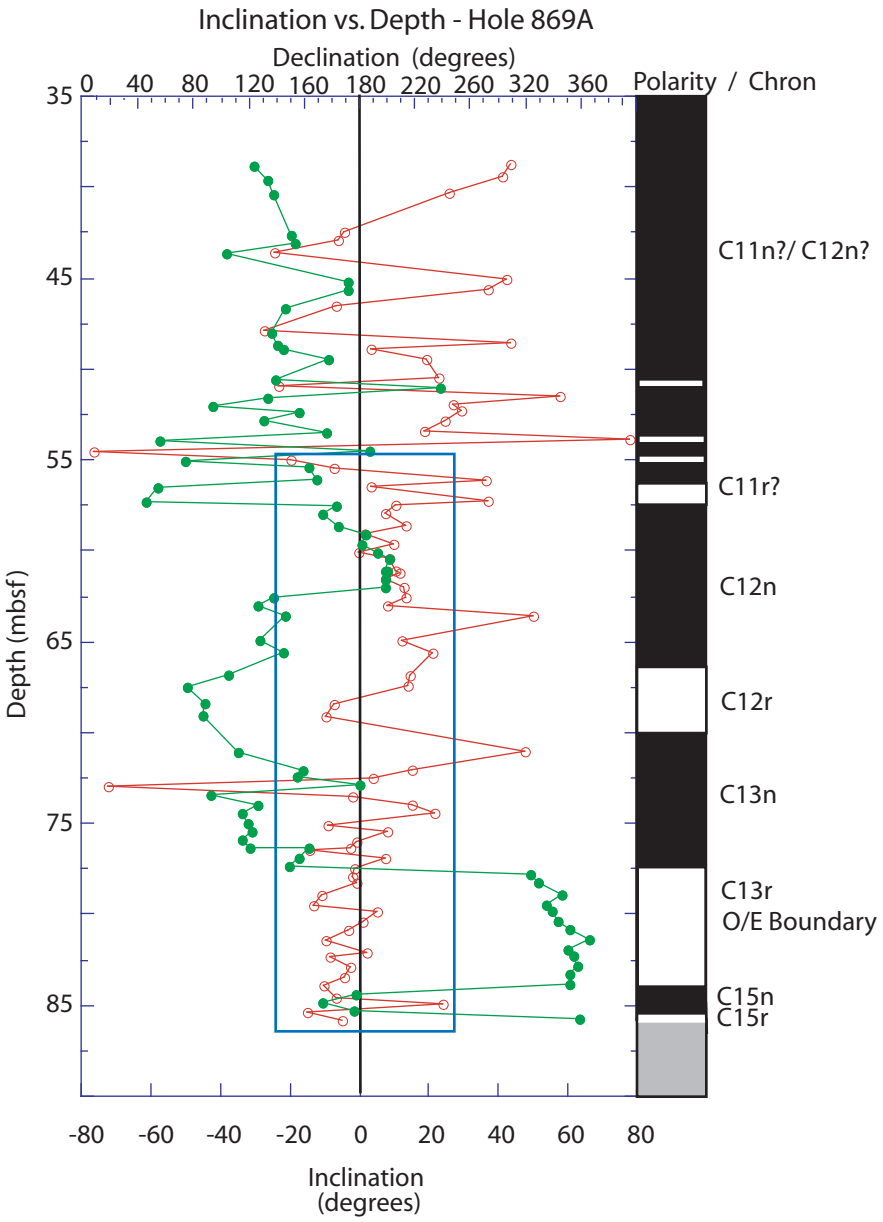


Figure A4. Magnetostratigraphy created for Leg 143 Hole 869A from discrete sediment samples of cores 143-896A-5H through 143-869A-9H. Polarity chron assignments based on biostratigraphy and ODP multishot tool corrected declinations [Firth, 1995; Shipboard Scientific Party, 1993; Gradstein et al., 2004]. Declination reversals used in place of inclinations to determine polarity due to proximity of site to equator. Open red circles denote inclination; filled green circles are corrected declination. Blue box shows data used to calculate mean colatitude.

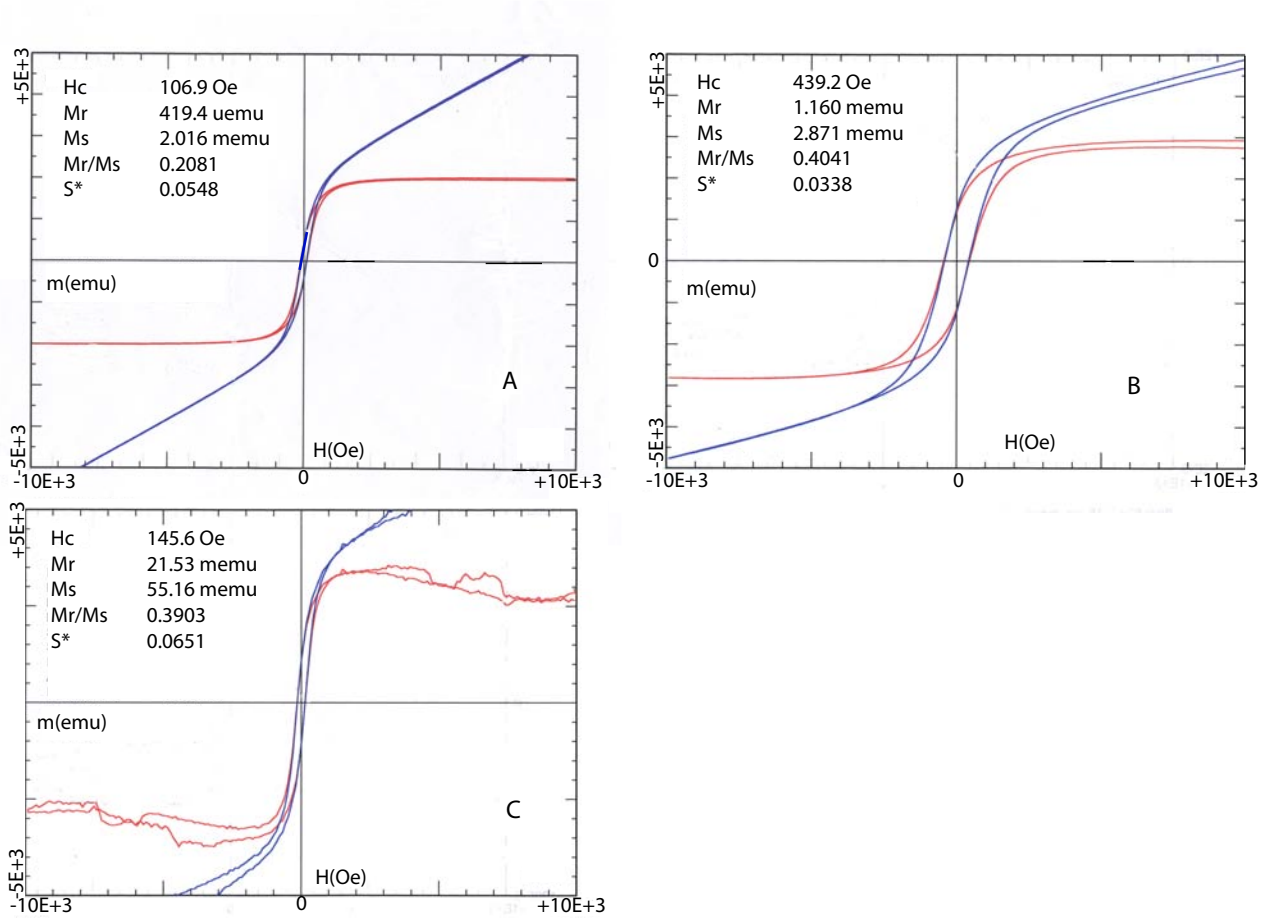


Figure A5. Selected examples of hysteresis analysis for Holes 884B and 869A. Hole 884B samples had higher magnetic intensities, producing results with less drift during analysis (A and B). Only a few Hole 869A samples were useable due to weak magnetic intensity and instrument noise. A) Sample 145-884B-70X-2, 40-42 cm; B) Sample 145-884B-83X-2, 15-17 cm; C) Sample 143-869A-5H-1, 27-29 cm. Narrow hysteresis loops (A and C) indicate presence of pseudo-single domain magnetite, (B) shows primarily pseudo-single domain with some single domain magnetite grains, evidenced by wider curve (wide curves characteristic of single domain grains). Blue curve is uncorrected data, red curve is de-trended.

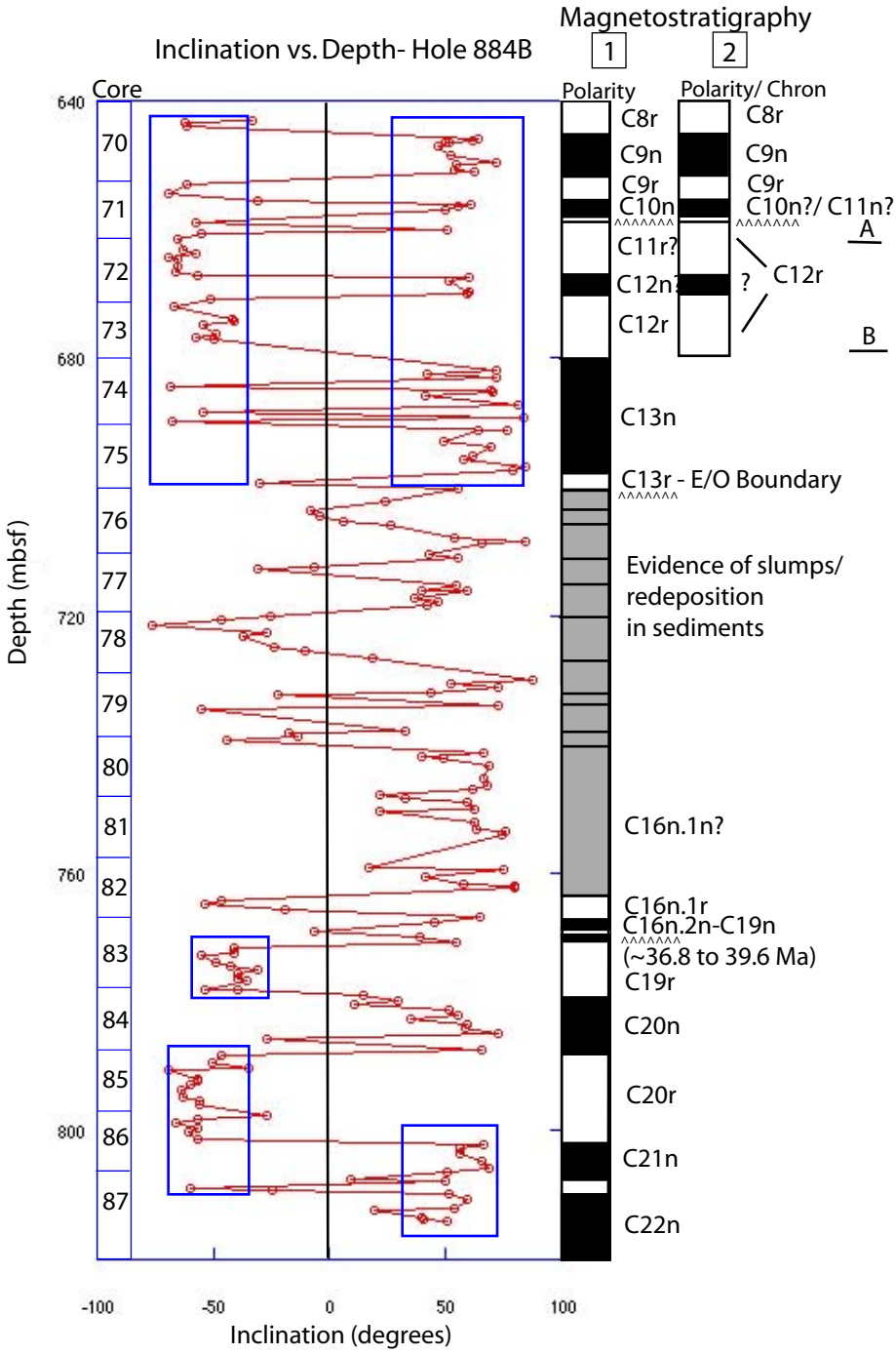


Figure A6. Leg 145 Hole 884B magnetostratigraphy compiled from biostratigraphy [Barron et al., 1995; Pak and Miller, 1995] and GPTS 2004 [Gradstein et al, 2004]. Upper section has two polarity interpretations; interpretation on left based on bio-stratigraphy and chron lengths; interpretation on right based on biostratigraphy. (A) represents first occurrence of *Rocella vigilans* and last occurrence (LO) of *Reticulofenestra umbilica* ~32.4 Ma; (B) is LO of *Ericsonia formosa*, ~33.2 Ma. Carrat symbols represent unconformities. Middle section interpretation of Hole 884B is unclear due to sediment slumping/redeposition. Blue boxes show data used to calculate mean colatitudes.

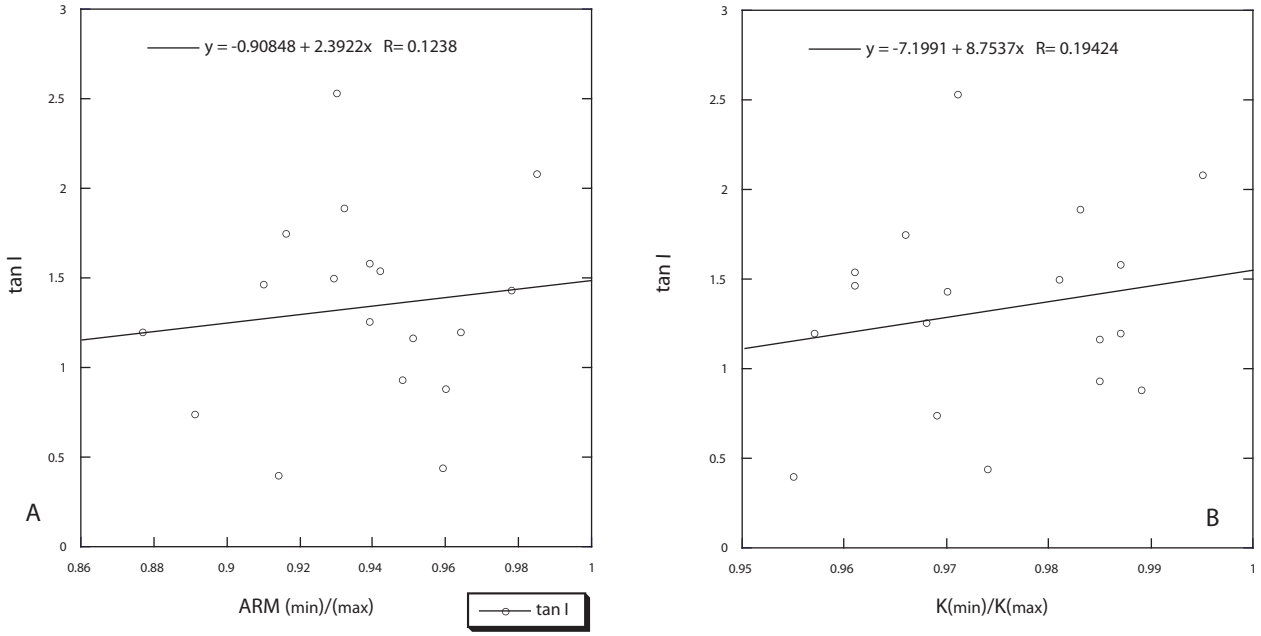


Figure A7. Plots of tan I versus ARM(min)/ARM(max) used for estimation of pre-inclination shallowing tan I values from the remanence inclinations of Hole 884B sediments. Predicted tan I located at intersection of regression line and ARM(min)/ARM(max) = 1 or K(min)/K(max) = 1. (A) method using ARM(min)/ARM(max) parameter from anhysteretic remanence and the tangents of the inclinations; (B) using susceptibilty value K(min)/K(max) from anisotropy (AMS) measurements and tan I.

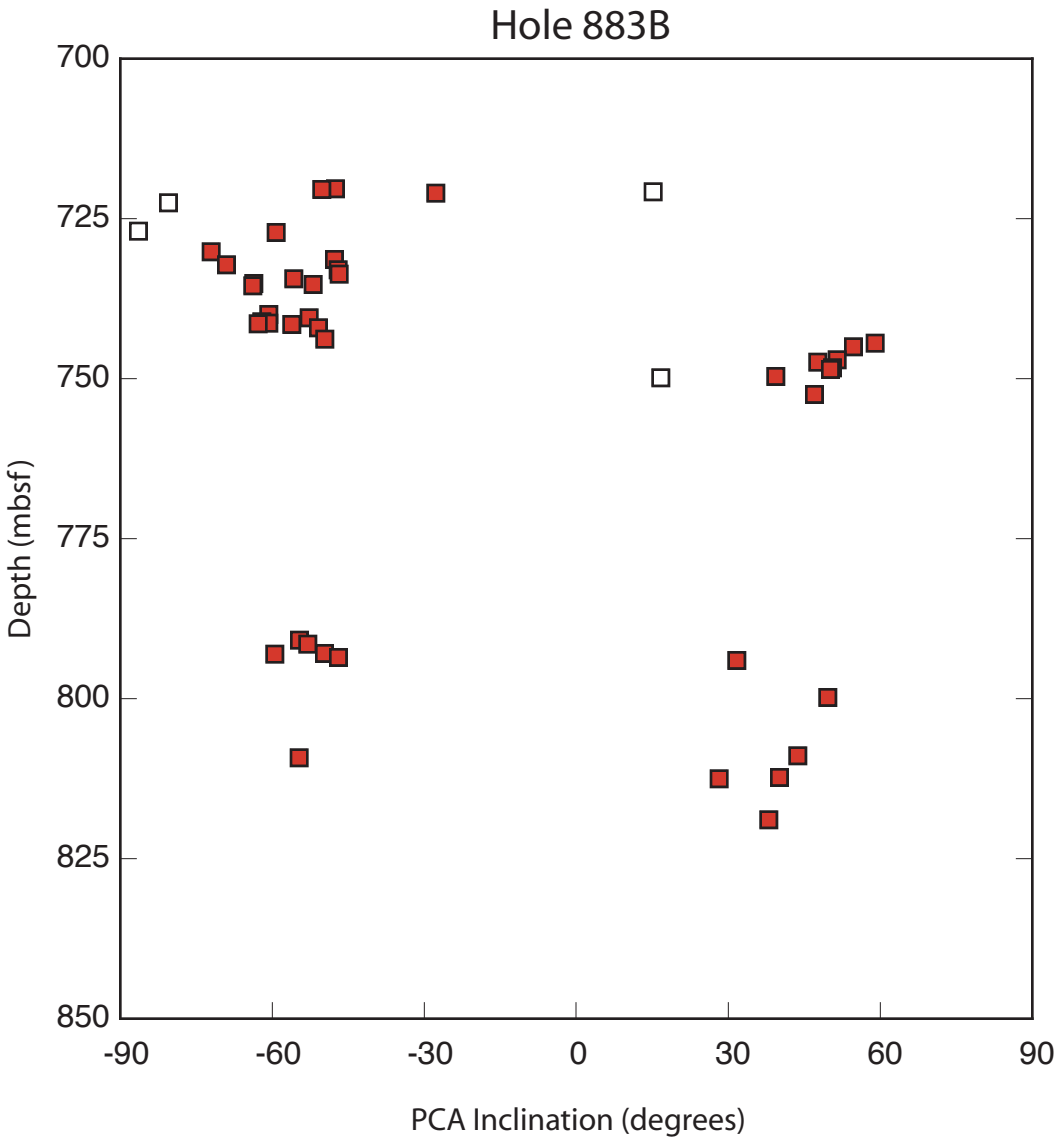


Figure A8. Plot of stable PCA inclination versus depth in meters below the seafloor for Eocene sediment samples from Hole 883B. Squares represent discrete sample inclinations; filled red squares are sample inclinations used to calculate mean paleocolatitude values.

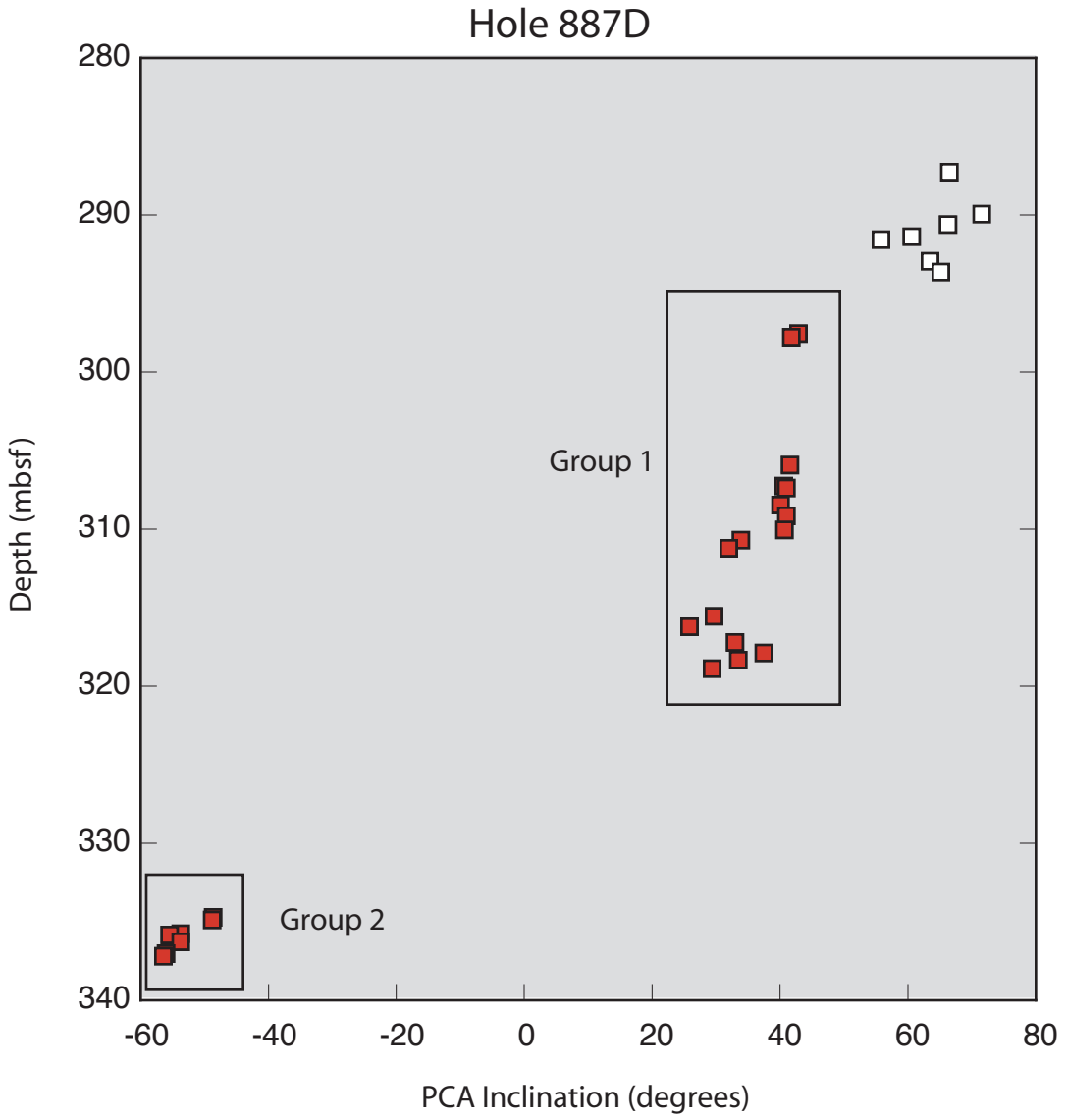


Figure A9. Plot of stable PCA inclination versus depth in meters below the seafloor for basalt samples from Hole 887D. Small squares represent discrete samples; red filled squares are samples used to calculate mean paleocolatitude. Large open boxes show inclination groupings of the igneous units used to average secular variation (SV).

A. Sample 200-1224F-04R-4, 4 cm (60.27 mbsf)

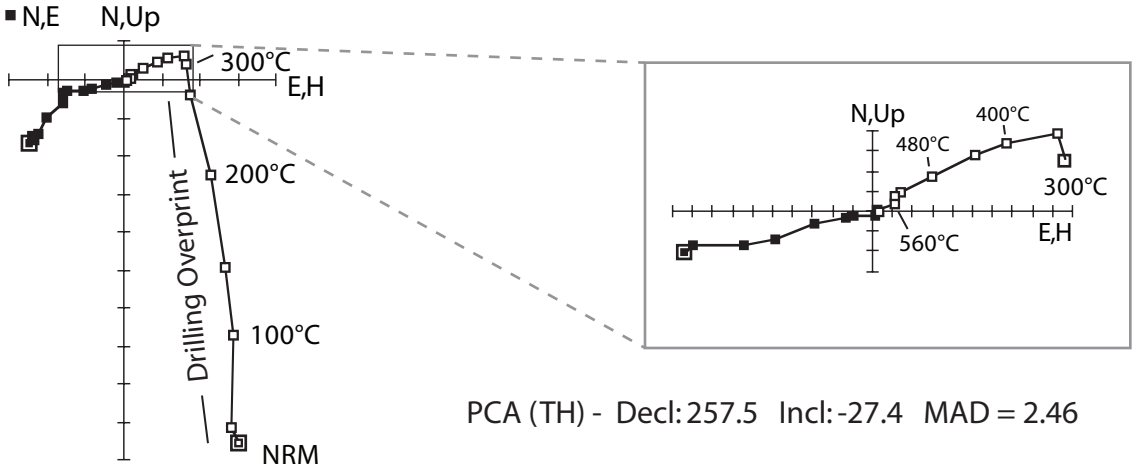


PCA (TH) - Decl: 257.5 Incl: -27.4 MAD = 2.46

B. Sample 200-1224F-14R-1, 48 cm (143.68 mbsf)

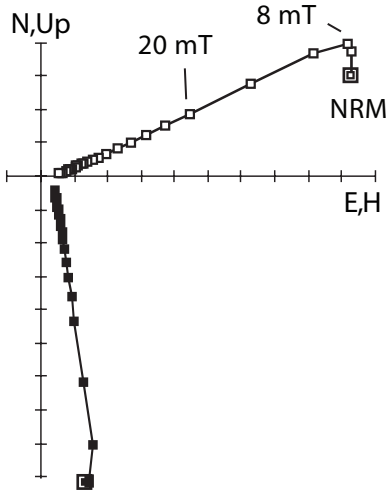


PCA (AF) - Decl: 171.1 Incl: -24.4 MAD = 1.36

Figure A10. Orthogonal vector demagnetization diagrams for (A) Sample 200-1224F-4R-4, 4 cm, from SV Unit 2, which was subjected to thermal demagnetization (TH) and (B) Sample 200-1224F-14R-1, 48 cm, from SV Unit 5, subjected to AF demagnetization (AF).

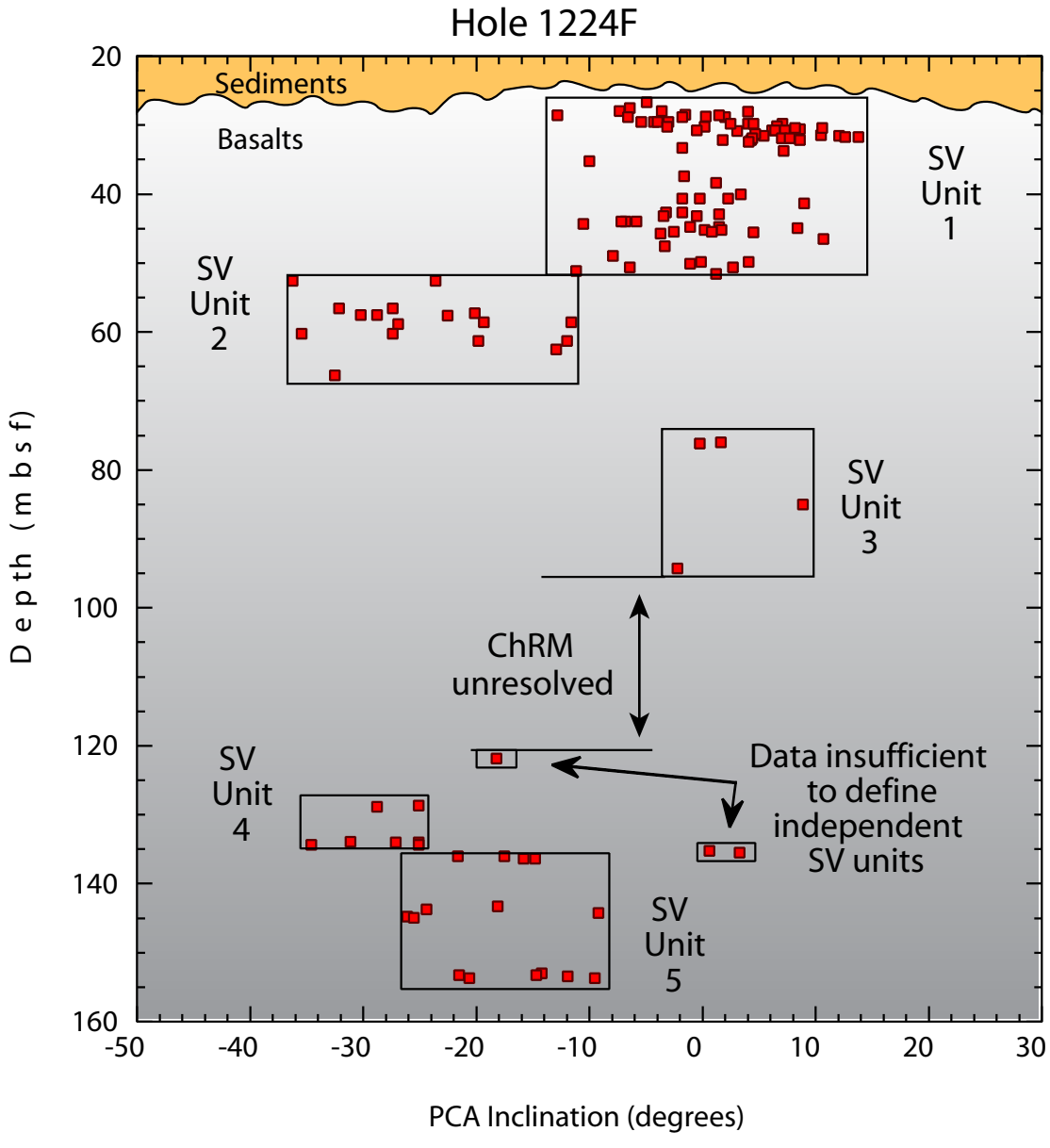


Figure A11. Plot of stable PCA inclination versus depth in meters below the seafloor for basalt samples from ODP Leg 200, Hole 1224F. Red squares represent discrete samples. Boxes show independent unit assignments for averaging secular variation (SV).

Table A1. Principle component analysis results of Leg 143 Hole 869A discrete sediment samples.

| Sample 143-869A- | Demag. levels | Declination (deg) | Corrected dec. (deg) | Inclination (deg) | MAD | A/UA | Consistency of data | Depth (mbsf) | Used in Colatitude |
|---|---|---|---|---|---|---|---|---|---|
| 05H1-027 | | ICA | | | | | F | 38.47 | N |
| 05H1-055 | 15-35 | 1.7 | 123.7 | 43.3 | 6.6 | A | B- | 38.75 | N |
| 05H1-126 | 15-35 | 12.0 | 134.0 | 40.8 | 6.7 | A | C | 39.46 | N |
| 05H2-010 | | ICA | | | | | F | 39.80 | N |
| 05H2-057 | 15-35 | 15.2 | 137.2 | 25.9 | 23.3 | A | C | 40.27 | N |
| 05H2-117 | | ICA | | | | | F | 40.87 | N |
| 05H3-010 | | ICA | | | | | F | 41.30 | N |
| 05H3-083 | | ICA | | | | | F | 42.03 | N |
| 05H3-129 | 15-35 | 28.3 | 150.3 | -4.2 | 9.8 | A | C | 42.49 | N |
| 05H4-024 | 15-35 | 31.6 | 153.6 | -6.1 | 10.3 | A | C | 42.94 | N |
| 05H4-083 | 15-35 | -19.1 | 102.9 | -24.3 | 6.3 | A | C | 43.53 | N |
| 05H4-133 | | ICA | | | | | F | 44.03 | N |
| 05H5-008 | | ICA | | | | | F | 44.28 | N |
| 05H5-088 | 15-25 | 69.3 | 191.3 | 42.5 | 20.2 | A | C | 45.08 | N |
| 05H5-142 | 15-30 | 69.7 | 191.7 | 36.9 | 11.8 | A | C | 45.62 | N |
| 05H6-021 | | ICA | | | | | F | 45.91 | N |
| 05H6-086 | 15-30 | 24.1 | 146.1 | -6.5 | 10.2 | A | B | 46.56 | Y |
| 05H6-136 | | ICA | | | | | F | 47.06 | N |
| 05H7-009 | | ICA | | | | | F | 47.29 | N |
| 05H7-054 | | ICA | | | | | F | 47.74 | N |
| 06H1-020 | 15-30 | -13.3 | 135.7 | -27.3 | 14.9 | A | C- | 47.90 | N |
| 06H1-086 | 15-25 | -8.5 | 140.5 | 43.1 | 22.8 | A | C | 48.56 | N |
| 06H1-116 | 15-25 | -4.5 | 144.5 | 3.5 | 24.7 | A | C | 48.86 | N |
| 06H2-020 | 15-25 | 28.4 | 177.4 | 19.3 | 24.2 | A | C- | 49.40 | N |
| 06H2-086 | | ICA | | | | | F | 50.06 | N |
| 06H2-132 | 15-25 | -10.7 | 138.3 | 23.0 | 20.9 | A | C- | 50.52 | N |
| 06H3-022 | 15-25 | 109.3 | 258.3 | -23.2 | 5.0 | A | C | 50.92 | N |
| 06H3-078 | 15-25 | -15.2 | 133.8 | 57.6 | 8.1 | A | B- | 51.48 | Y |
| 06H3-126 | 10 to 30 | 305.3 | 94.3 | 27.0 | 11.9 | UA | C | 51.96 | N |
| 06H4-011 | 15-30 | 6.9 | 155.9 | 29.1 | 13.1 | A | C | 52.31 | N |
| 06H4-061 | 20-40 | -19.2 | 129.8 | 24.7 | 28.5 | UA | C | 52.81 | N |
| 06H4-125 | 15-30 | 26.3 | 175.3 | 18.8 | 18.9 | A | C- | 53.45 | N |
| 06H5-018 | 15-30 | 265.7 | 54.7 | 77.4 | 3.6 | A | C | 53.88 | N |
| 06H5-079 | 15-35 | 57.9 | 206.9 | -76.6 | 12.5 | A | C- | 54.49 | N |
| 06H5-128 | 15-35 | 284.2 | 73.2 | -19.9 | 7.8 | A | B | 54.98 | Y |
| 06H6-020 | 20,30,35 | 14.1 | 163.1 | -7.6 | 11.3 | UA | C | 55.40 | N |
| 06H6-088 | 15-25,35 | 20.4 | 169.4 | 36.2 | 8.3 | A | C | 56.08 | N |
| 06H6-130 | 25-35 | 264.7 | 53.7 | 3.2 | 12.7 | UA | B | 56.50 | Y |
| 06H7-007 | | ICA | | | | | F | 56.77 | N |
| 06H7-060 | 20-30 | 256.7 | 45.7 | 36.7 | 13.3 | A | C | 57.30 | N |
| 07H2-015 | 20-30 | 196.5 | 182.5 | 10.2 | 6.1 | A | B | 57.47 | Y |
| 07H2-064 | 15-35 | 186.8 | 172.8 | 7.6 | 5.2 | UA | B | 57.96 | Y |
| 07H2-134 | 15-35 | 197.7 | 183.7 | 13.0 | 2.8 | A | B | 58.66 | Y |
| 07H3-027 | 15-35 | 218.6 | 204.6 | 1.7 | 4.2 | A | B | 59.09 | Y |
| 07H3-084 | 15-25 | 214.9 | 200.9 | 9.9 | 1.0 | A | B | 59.66 | Y |
| 07H3-128 | 15-25 | 226.1 | 212.1 | -0.4 | 1.0 | A | B+ | 60.10 | Y |
| 07H4-012 | 15-25 | 234.7 | 220.7 | 8.5 | 0.5 | A | B+ | 60.44 | Y |
| 07H4-075 | 20-35 | 233.0 | 219.0 | 10.5 | 4.6 | UA | A | 61.07 | Y |
| 07H4-083 | 15-25 | 234.2 | 220.2 | 11.3 | 1.9 | UA | A | 61.15 | Y |
| 07H4-125 | 15-25 | 232.3 | 218.3 | 7.3 | 1.0 | A | B+ | 61.57 | Y |
| 07H5-018 | 15-25 | 232.3 | 218.3 | 12.7 | 1.8 | A | B | 62.00 | Y |

Table A1. Continued.

| Sample 143-869A- | Demag. Levels | Declination (deg) | Corrected Dec. (deg) | Inclination (deg) | MAD | A/UA | Consistency of data | Depth (mbsf) | Used in Colatitude |
|---|---|---|---|---|---|---|---|---|---|
| 07H5-070 | 15-25 | 151.5 | 137.5 | 13.4 | 14.4 | A | C | 62.52 | N |
| 07H5-114 | 15-30 | 140.3 | 126.3 | 8.2 | 15.6 | A | C | 62.96 | N |
| 07H6-023 | 15-25 | 160.4 | 146.4 | 49.6 | 10.1 | A | C- | 63.55 | N |
| 07H6-070 | | ICA | | | | | F | 64.02 | N |
| 07H6-132 | | ICA | | | | | F | 64.64 | N |
| 07H7-015 | 15-30 | 141.2 | 127.2 | 11.9 | 38.9 | A | C- | 64.97 | N |
| 07H7-075 | 20-30 | 158.0 | 144.0 | 20.7 | 8 | A | C | 65.57 | N |
| 07H7-140 | | ICA | | | | | F | 66.22 | N |
| 07H8-014 | | ICA | | | | | F | 66.46 | N |
| 07H8-054 | 15-30 | 119.4 | 105.4 | 14.7 | 7.5 | A | B- | 66.86 | Y |
| 08H2-018 | | ICA | | | | | F | 66.93 | N |
| 08H2-071 | 15-30 | 82.0 | 75.0 | 13.9 | 4.3 | A | B | 67.46 | Y |
| 08H2-125 | | ICA | | | | | F | 68.00 | N |
| 08H3-015 | 15-30 | 95.5 | 88.5 | -7.1 | 11.8 | A | C | 68.40 | N |
| 08H3-047 | | ICA | | | | | F | 68.72 | N |
| 08H3-088 | 20-35 | 93.0 | 86.0 | -9.9 | 6.9 | A | B | 69.13 | Y |
| 08H4-049 | | ICA | | | | | F | 70.24 | N |
| 08H4-088 | | ICA | | | | | F | 70.63 | N |
| 08H4-131 | 15-25 | 119.6 | 112.6 | 47.3 | 8.3 | A | C | 71.06 | N |
| 08H5-017 | | ICA | | | | | F | 71.42 | N |
| 08H5-082 | 15-25 | 165.2 | 158.2 | 14.8 | 7.9 | A | C | 72.07 | N |
| 08H5-122 | 15-30 | 162.2 | 155.2 | 3.7 | 17.5 | A | C | 72.45 | N |
| 08H6-017 | 15-35 | 206.6 | 199.6 | -72.3 | 10.4 | UA | B- | 72.92 | N |
| 08H6-077 | 15-25 | 99.2 | 92.2 | -2.2 | 8.4 | A | C | 73.52 | N |
| 08H6-125 | 15-35 | 133.0 | 126.0 | 14.9 | 4.3 | UA | A | 74.00 | Y |
| 08H7-020 | 15-35 | 122.3 | 115.3 | 21.7 | 6.5 | UA | B | 74.45 | Y |
| 08H7-082 | 20-35 | 126.2 | 119.2 | -9.0 | 8.8 | UA | A- | 75.07 | Y |
| 08H7-120 | 15-35 | 128.7 | 121.7 | 7.8 | 3.3 | A | B | 75.45 | Y |
| 08H8-019 | 20-35 | 121.6 | 114.6 | -0.7 | 1.9 | A | B+ | 75.94 | Y |
| 08H8-063 | 15-35 | 127.0 | 120.0 | -2.6 | 2.9 | A | B | 76.38 | Y |
| 09H1-024 | 15-35 | 188.4 | 163.4 | -14.4 | 3.5 | A | B | 76.44 | Y |
| 09H1-071 | 15-35 | 180.4 | 155.4 | 7.6 | 2.7 | A | B | 76.91 | Y |
| 09H1-123 | 15-35 | 174.0 | 149.0 | -1.6 | 5.3 | UA | A | 77.43 | Y |
| 09H2-016 | 15-30 | -11.5 | 323.5 | -1.9 | 3.2 | UA | A | 77.86 | Y |
| 09H2-059 | 15-35 | -5.4 | 329.6 | -0.9 | 3.7 | UA | A | 78.29 | Y |
| 09H2-123 | 15-30 | 11.0 | 346.0 | -11.2 | 1.6 | A | B | 78.93 | Y |
| 09H3-030 | 20-40 | -0.1 | 334.9 | -13.3 | 4.9 | UA | A | 79.50 | Y |
| 09H3-068 | 15-35 | 4.2 | 339.2 | 5.2 | 1.1 | UA | B | 79.88 | Y |
| 09H3-124 | 15-25 | 8.9 | 343.9 | 0.9 | 1.5 | A | B+ | 80.44 | Y |
| 09H4-014 | 15-35 | 17.2 | 352.2 | -3.3 | 5.5 | UA | B | 80.84 | Y |
| 09H4-070 | 15-35 | 30.6 | 365.6 | -9.8 | 3.1 | UA | A | 81.40 | Y |
| 09H4-135 | 15-35 | 15.1 | 350.1 | 1.9 | 4.6 | UA | B+ | 82.05 | Y |
| 09H5-013 | 15-35 | 19.0 | 354.0 | -8.7 | 2.2 | UA | B+ | 82.33 | Y |
| 09H5-071 | 15-35 | 22.4 | 357.4 | -2.4 | 1.2 | A | A- | 82.91 | Y |
| 09H5-120 | 15-35 | 17.2 | 352.2 | -4.2 | 2 | UA | B+ | 83.40 | Y |
| 09H6-018 | 15-35 | 16.5 | 351.5 | -10.1 | 1.5 | A | B+ | 83.88 | Y |
| 09H6-084 | 15-35 | 221.6 | 196.6 | -6.9 | 8.7 | A | B- | 84.54 | Y |
| 09H6-123 | 15-35 | 197.7 | 172.7 | 23.7 | 3.9 | UA | A | 84.93 | Y |
| 09H7-017 | 15-35 | 220.4 | 195.4 | -15.2 | 2.7 | A | B | 85.37 | Y |
| 09H7-063 | 20-35 | 24.0 | 359.0 | -5.0 | 2.4 | A | B- | 85.83 | Y |

*Abbreviations:* Demag. Levels= demagnetization steps used for PCA calculation; ICA= Inconsistent directions; A/UA= Anchored/Unanchored fit of PCA to (0,0); MAD= Maximum Angular Deviation of PCA; Consistency of data= Consistency of directions with PCA solution inclinations (range: A=excellent to F=poor). Declination corrections= Core 5H (+122 deg), Core 6H (+149 deg), Core 7H (+346 deg), Core 8H (+353 deg), Core 9H (+335 deg).

Table A2. Principle component analysis results of Leg 145 Hole 884B discrete sediment samples.

| Sample 145-884B- | Demag. levels | Declination (deg) | Inclination (deg) | MAD | A/UA | Consistency of data | Depth (mbsf) | Used in colatitude |
|---|---|---|---|---|---|---|---|---|
| 70X1-121 | 10-50 | 303.2 | -33.6 | 2.8 | A | B | 643.21 | N |
| 70X1-147 | 5-50 | 51.2 | -62.1 | 1.4 | A | A- | 643.47 | Y |
| 70X2-040 | 5-50 | 173.8 | -61.4 | 2.8 | UA | A- | 643.90 | Y |
| 70X3-082 | 10-35 | 25.5 | 64.1 | 2.4 | A | B | 645.82 | Y |
| 70X3-133 | 5-35 | 70.6 | 61.7 | 2.1 | A | B | 646.33 | Y |
| 70X3-144 | 5-40 | 156.3 | 51.5 | 2.7 | UA | B+ | 646.44 | Y |
| 70X4-008 | 15-40 | 161.6 | 50.0 | 2.7 | UA | A- | 646.58 | Y |
| 70X4-070 | 20-60 | 70.3 | 46.6 | 3.5 | UA | B | 647.20 | Y |
| 70X5-059 | 5-50 | 84.7 | 52.1 | 2.9 | UA | A | 648.59 | Y |
| 70X5-109 | 10-50 | -36.8 | 71.9 | 1.6 | UA | A | 649.59 | Y |
| 70X6-041 | 5-50 | 198.5 | 54.8 | 1.1 | UA | A | 649.91 | Y |
| 70X6-120 | 5-50 | 194.8 | 53.8 | 1.1 | A | A | 650.70 | Y |
| 70X7-011 | 10-50 | 29.3 | 62.3 | 3.2 | A | B+ | 651.11 | Y |
| 71X1-139 | 10-50 | 164.7 | -61.2 | 1.9 | UA | A | 653.09 | Y |
| 71X2-133 | 10-50 | 172.2 | -69.4 | 0.4 | UA | A | 654.53 | Y |
| 71X3-081 | 15-50 | -17.3 | -31.2 | 3.2 | A | B+ | 655.51 | Y |
| 71X3-145 | 5-50 | 53.7 | 60.5 | 1.9 | UA | A | 656.15 | Y |
| 71X4-013 | 10-50 | 264.8 | 55.4 | 1.0 | UA | A | 656.33 | Y |
| 71X4-072 | 5-50 | 144.5 | 49.5 | 0.8 | UA | A- | 656.92 | Y |
| 71X5-114 | 10-50 | 127.4 | -58.0 | 2.3 | UA | A- | 658.84 | Y |
| 71X6-081 | 5-50 | -12.8 | 50.8 | 1.2 | UA | A | 660.01 | Y |
| 71X7-010 | 10-50 | 151.7 | -55.4 | 2.0 | UA | A | 660.80 | Y |
| 72X1-015 | 10-60 | 166.0 | -65.5 | 2.1 | A | B+ | 661.45 | Y |
| 72X2-043 | 10-50 | 272.5 | -63.3 | 2.8 | A | B | 663.23 | Y |
| 72X2-100 | 10-50 | 33.9 | -57.6 | 2.2 | UA | A- | 663.80 | Y |
| 72X2-144 | 10-50 | 208.0 | -69.2 | 2.9 | UA | A- | 664.24 | Y |
| 72X3-046 | 5-50 | 187.3 | -65.3 | 2.3 | UA | A | 664.76 | Y |
| 72X3-144 | 5-50 | 258.8 | -65.6 | 1.4 | UA | A | 665.74 | Y |
| 72X4-074 | 15-50 | 328.7 | -66.6 | 2.4 | A | B+ | 666.54 | Y |
| 72X4-131 | 10-50 | 90.2 | -56.5 | 2.0 | UA | B+ | 667.11 | Y |
| 72X5-019 | 10-50 | 146.4 | 60.3 | 0.7 | UA | A- | 667.49 | Y |
| 72X5-072 | 10-50 | 233.8 | 51.3 | 1.6 | UA | A | 668.02 | Y |
| 72X6-105 | 10-50 | -84.0 | 60.3 | 1.3 | UA | A | 669.85 | Y |
| 72X6-129 | 10-50 | -30.6 | 59.4 | 2.4 | UA | A | 670.09 | Y |
| 72X7-051 | 10-50 | 60.4 | -51.1 | 1.8 | UA | A | 670.81 | Y |
| 73X1-084 | 10-60 | 215.8 | -67.3 | 1.2 | UA | A | 671.84 | Y |
| 73X2-134 | 10-50 | 128.7 | -42.2 | 2.2 | UA | A- | 673.84 | Y |
| 73X3-014 | 10-50 | -2.3 | -41.4 | 1.7 | UA | A | 674.14 | Y |
| 73X3-068 | 10-50 | 289.4 | -54.8 | 1.3 | UA | A- | 674.68 | Y |
| 73X4-060 | 10-50 | 47.9 | -49.4 | 1.1 | A | B+ | 676.10 | Y |
| 73X4-123 | 10-50 | 28.4 | -57.5 | 1.5 | UA | A | 676.73 | Y |
| 73X5-012 | 10-50 | 153.4 | -50.1 | 1.6 | UA | A | 677.12 | Y |
| 74X1-105 | | ICA | | | | F | 681.65 | N |
| 74X1-129 | 15-40 | 130.6 | 72.1 | 2.9 | A | B- | 681.89 | Y |
| 74X2-022 | 15-40 | 164.6 | 41.9 | 5.4 | A | B- | 682.32 | Y |
| 74X2-111 | 15-35 | 133.4 | 72.0 | 6.1 | A | C | 683.11 | N |
| 74X3-071 | 15-30 | 101.6 | -68.4 | 4.6 | A | C | 684.31 | N |
| 74X3-138 | 10-50 | 231.8 | 69.3 | 1.8 | A | B | 684.98 | Y |
| 74X4-020 | 10-50 | 103.7 | 70.3 | 1.8 | UA | B+ | 685.30 | Y |
| 74X4-078 | 15-50 | 152.9 | 40.9 | 7.7 | A | C | 685.88 | N |
| 74X5-064 | 10-50 | 120.4 | 80.8 | 1.5 | A | B+ | 687.24 | N |
| 74X6-020 | 10-50 | 294.6 | -54.3 | 6.2 | A | B- | 688.30 | Y |

Table A2. Continued.

| Sample 145-884B- | Demag. levels | Declination (deg) | Inclination (deg) | MAD | A/UA | Consistency of data | Depth (mbsf) | Used in colatitude |
|---|---|---|---|---|---|---|---|---|
| 74X6-101 | 15-40 | 172.0 | 83.9 | 1.1 | A | B | 689.11 | N |
| 74X7-008 | 10-50 | 206.0 | -68.1 | 1.3 | A | B+ | 689.68 | Y |
| 75X1-096 | 10-50 | 197.5 | 76.3 | 3.2 | A | B- | 691.16 | N |
| 75X1-115 | 10-50 | 12.5 | 64.3 | 4.2 | A | B | 691.35 | Y |
| 75X2-113 | 10-50 | 170.5 | 49.1 | 4.8 | A | B- | 692.83 | Y |
| 75X3-067 | 5-40 | 236.5 | 69.8 | 3.4 | A | B | 693.87 | Y |
| 75X3-083 | | ICA | | | | F | 694.03 | N |
| 75X4-044 | 10-35 | 222.6 | 61.6 | 11.5 | A | C | 695.14 | N |
| 75X4-102 | 10-35 | 2.1 | 57.5 | 6.0 | A | C | 695.72 | N |
| 75X5-066 | 10-50 | -14.9 | 84.7 | 2.2 | A | B+ | 696.86 | N |
| 75X5-124 | 10-20,30-40 | 195.8 | 78.8 | 3.8 | A | C | 697.44 | N |
| 75X6-026 | | ICA | | | | F | 697.96 | N |
| 75X6-046 | | ICA | | | | F | 698.16 | N |
| 75X7-004 | | ICA | | | | F | 698.74 | N |
| 75X7-079 | 10-20,30-50 | 118.3 | -30.5 | 2.3 | A | B | 699.49 | N |
| 76X1-041 | 5-35 | 62.6 | 55.0 | 4.8 | A | C- | 700.21 | N |
| 76X2-084 | 10-20,30-50 | 102.3 | 23.8 | 3.7 | A | B- | 702.14 | N |
| 76X3-086 | 10-20,30-50 | -33.2 | -8.6 | 5.8 | A | C | 703.66 | N |
| 76X4-027 | 15-40 | -21.2 | -4.7 | 3.2 | A | B- | 704.57 | N |
| 76X4-110 | 5-50 | 145.1 | 5.9 | 3.9 | A | B | 705.40 | N |
| 76X5-005 | 15-40 | 152.8 | 26.5 | 4.6 | A | B- | 705.85 | N |
| 76X6-071 | 15-40 | 29.0 | 53.8 | 3.0 | A | B | 708.01 | N |
| 76X6-106 | 10-50 | -87.1 | 84.2 | 1.9 | A | B+ | 708.36 | N |
| 76X7-009 | 10-50 | 258.6 | 65.4 | 1.3 | A | B+ | 708.89 | N |
| 77X1-101 | 10-60 | -58.8 | 42.5 | 6.9 | A | C+ | 710.51 | N |
| 77X2-008 | 10-50 | 221.8 | 55.2 | 1.6 | A | B+ | 711.08 | N |
| 77X2-144 | 15-50 | 84.5 | -6.9 | 2.5 | A | B | 712.44 | N |
| 77X3-021 | 15-50 | -43.6 | -30.6 | 1.7 | A | B+ | 712.71 | N |
| 77X4-122 | 15-50 | 200.7 | 54.7 | 3.3 | UA | B- | 715.22 | N |
| 77X5-056 | 5-30,40 | 189.6 | 39.9 | 2.3 | A | B- | 716.06 | N |
| 77X5-064 | 10-50 | 60.9 | 58.9 | 6.4 | A | B- | 716.14 | N |
| 77X6-023 | 15-35 | 131.7 | 36.4 | 4.3 | A | B- | 717.23 | N |
| 77X6-085 | 10-30 | -85.2 | 46.7 | 1.5 | A | B | 717.85 | N |
| 77X6-142 | 10-50 | 311.0 | 41.8 | 2.3 | UA | A- | 718.42 | N |
| 78X1-086 | 10-50 | 171.7 | -25.6 | 2.7 | A | B | 719.96 | N |
| 78X2-013 | 15-50 | 250.4 | -46.7 | 4.2 | A | B | 720.73 | N |
| 78X2-091 | 10-50 | 279.7 | -76.3 | 2.2 | A | B+ | 721.51 | N |
| 78X3-048 | 10-50 | 203.4 | -26.8 | 2.5 | UA | A- | 722.58 | N |
| 78X3-107 | 15-50 | 154.4 | -36.9 | 4.5 | UA | B+ | 723.17 | N |
| 78X4-143 | 15-40 | 42.9 | -23.6 | 4.0 | A | B- | 725.03 | N |
| 78X5-027 | 5-35,50 | 26.6 | -10.3 | 4.6 | A | B | 725.37 | N |
| 78X6-007 | 15-50 | -12.5 | 18.5 | 1.9 | A | B | 726.67 | N |
| 79X1-022 | | ICA | | | | F | 729.02 | N |
| 79X1-108 | 15-50 | -53.2 | 87.1 | 5.5 | A | C- | 729.88 | N |
| 79X2-028 | 20-40 | 103.4 | 52.2 | 10.5 | A | C- | 730.58 | N |
| 79X2-073 | 20-50 | 220.0 | 72.5 | 10.5 | A | C- | 731.03 | N |
| 79X3-010 | 20-40 | 163.0 | 43.7 | 5.6 | A | C | 731.90 | N |
| 79X3-054 | 15-25,35 | 204.3 | -22.1 | 6.9 | A | C | 732.34 | N |
| 79X4-060 | 15-35 | 80.6 | 72.7 | 9.7 | A | C- | 733.90 | N |
| 79X4-124 | 15-40 | 55.0 | -55.4 | 3.2 | A | C+ | 734.54 | N |
| 79X5-082 | | ICA | | | | F | 735.62 | N |
| 79X5-120 | | ICA | | | | F | 736.00 | N |
| 79X6-081 | | ICA | | | | F | 737.11 | N |

Table A2. Continued.

| Sample 145-884B- | Demag. levels | Declination (deg) | Inclination (deg) | MAD | A/UA | Consistency of data | Depth (mbsf) | Used in colatitude |
|---|---|---|---|---|---|---|---|---|
| 79X7-011 | 20-50 | 211.2 | 32.7 | 2.6 | A | B | 737.91 | N |
| 79X7-041 | 25-40 | 196.7 | -17.5 | 3.7 | A | B- | 738.21 | N |
| 80X1-046 | 25-40 | 66.4 | -13.5 | 4.9 | A | D | 738.86 | N |
| 80X1-093 | 15-50 | 27.1 | -44.0 | 4.2 | A | C | 739.33 | N |
| 80X2-072 | | ICA | | | | F | 740.62 | N |
| 80X2-128 | 20-60 | -3.6 | 66.5 | 2.9 | UA | B+ | 741.18 | N |
| 80X3-041 | 20-40 | 221.7 | 39.5 | 3.8 | A | B- | 741.81 | N |
| 80X3-077 | 15-40 | 192.3 | 49.1 | 2.5 | A | B+ | 742.17 | N |
| 80X4-051 | 25-50 | -5.2 | 68.7 | 13.8 | A | C | 743.41 | N |
| 80X4-116 | | ICA | | | | F | 744.06 | N |
| 80X5-086 | 20-60 | 135.0 | 66.0 | 10.6 | A | C | 745.26 | N |
| 80X5-120 | | ICA | | | | F | 745.60 | N |
| 80X6-063 | 25-60 | 150.5 | 67.7 | 11.0 | A | C- | 746.53 | N |
| 80X6-097 | 15-35 | 104.5 | 61.6 | 7.8 | A | C | 746.87 | N |
| 80X7-054 | 10-40 | 182.8 | 21.5 | 3.4 | A | B | 747.94 | N |
| 81X1-032 | 15-35 | -35.6 | 32.2 | 4.9 | A | C+ | 748.42 | N |
| 81X1-081 | 5-20 | 116.3 | 59.5 | 2.5 | A | C | 748.91 | N |
| 81X2-053 | 10-25 | 191.6 | 62.0 | 8.1 | A | C- | 750.13 | N |
| 81X2-081 | 10-40 | 192.2 | 21.9 | 2.4 | A | B | 750.41 | N |
| 81X3-051 | | ICA | | | | F | 751.61 | N |
| 81X3-102 | 10-30 | 132.4 | 62.4 | 5.5 | A | C | 752.12 | N |
| 81X4-071 | 20-50 | 195.2 | 62.8 | 9.1 | A | C- | 753.31 | N |
| 81X4-083 | 10-50 | 4.3 | 75.3 | 2.1 | UA | A- | 753.43 | N |
| 81X5-009 | 10-40 | 0.4 | 73.8 | 3.0 | A | B | 754.19 | N |
| 82X1-047 | | ICA | | | | F | 758.17 | N |
| 82X1-135 | 25-80 | 14.4 | 16.9 | 4.0 | A | B- | 759.05 | N |
| 82X2-023 | 15-40 | 25.5 | 74.8 | 3.2 | A | B- | 759.43 | N |
| 82X2-143 | 15-80 | 142.4 | 41.2 | 1.9 | UA | A | 760.63 | N |
| 82X3-090 | 15-80 | 249.0 | 57.3 | 1.2 | A | B+ | 761.60 | N |
| 82X3-136 | 15-80 | 136.4 | 79.6 | 0.6 | A | B+ | 762.06 | N |
| 82X4-005 | 15-80 | -60.5 | 79.3 | 0.8 | A | B++ | 762.25 | N |
| 82X4-068 | | ICA | | | | F | 762.88 | N |
| 82X5-060 | 20-80 | 241.1 | -46.8 | 1.2 | UA | A | 764.30 | N |
| 82X5-101 | 20-80 | 282.3 | -53.7 | 1.3 | UA | B+ | 764.71 | N |
| 82X6-048 | 25-80 | 308.5 | -19.3 | 0.8 | UA | A | 765.68 | N |
| 82X7-012 | 10-25 | 167.4 | 64.9 | 5.1 | A | C | 766.82 | N |
| 83X1-011 | 15-25 | -46.6 | 44.9 | 3.8 | A | C- | 767.51 | N |
| 83X2-015 | 50-80 | -1.5 | -7.0 | 1.6 | A | C | 769.05 | N |
| 83X2-101 | 15-30 | 207.8 | 39.2 | 4.2 | A | C | 769.91 | N |
| 83X3-043 | 15-30 | 259.9 | 54.9 | 3.1 | A | C | 770.83 | N |
| 83X3-116 | 35-80 | 282.4 | -41.3 | 2.9 | A | B | 771.56 | Y |
| 83X4-062 | 40-80 | 328.0 | -40.8 | 0.7 | A | B+ | 772.52 | Y |
| 83X4-072 | 25-80 | 353.3 | -55.5 | 1.5 | A | B- | 772.62 | Y |
| 83X5-036 | 5-50 | 223.9 | -48.8 | 1.0 | UA | B+ | 773.76 | Y |
| 83X5-091 | 10-60 | 20.1 | -43.0 | 1.1 | UA | B | 774.31 | Y |
| 83X6-015 | 20-80 | 87.0 | -30.9 | 1.3 | A | B | 775.05 | Y |
| 83X6-070 | 15-80 | -5.8 | -39.3 | 0.3 | A | B+ | 775.60 | Y |
| 83X7-014 | 35-80 | 140.0 | -39.6 | 0.6 | A | B+ | 776.54 | Y |
| 83X7-032 | 25-80 | 144.7 | -35.4 | 0.7 | A | B+ | 776.72 | Y |
| 84X1-101 | 30-80 | 217.1 | -53.7 | 1.9 | A | B | 778.01 | Y |
| 84X1-116 | 25-80 | 35.0 | -39.6 | 0.7 | A | B+ | 778.16 | Y |
| 84X2-059 | 30-80 | 175.2 | 14.3 | 5.0 | A | C | 779.09 | N |
| 84X2-129 | 25-80 | 295.1 | 29.6 | 0.6 | A | B+ | 779.79 | N |

Table A2. Continued.

| Sample 145-884B- | Demag. levels | Declination (deg) | Inclination (deg) | MAD | A/UA | Consistency of data | Depth (mbsf) | Used in colatitude |
|---|---|---|---|---|---|---|---|---|
| 84X3-031 | 15-80 | 116.0 | 10.6 | 0.9 | A | B+ | 780.31 | N |
| 84X3-119 | 25-80 | 181.7 | 51.1 | 1.3 | A | B- | 781.19 | N |
| 84X4-061 | 30-80 | 11.4 | 55.3 | 4.1 | A | C+ | 782.11 | N |
| 84X4-113 | 15-80 | 189.9 | 35.1 | 1.4 | A | B+ | 782.63 | N |
| 84X5-045 | 10-35 | 36.2 | 59.5 | 2.4 | A | B- | 783.45 | N |
| 84X5-106 | 10-30 | 237.9 | 58.3 | 8.2 | A | C | 784.06 | N |
| 84X6-043 | 10-40 | 85.8 | 72.9 | 4.3 | A | B- | 784.93 | N |
| 84X6-123 | 10-35 | 293.8 | -27.3 | 1.9 | UA | B | 785.73 | N |
| 84X7-026 | | ICA | | | | F | 786.26 | N |
| 85X1-029 | | ICA | | | | F | 786.99 | N |
| 85X1-062 | 10-25 | 222.3 | 65.3 | 0.7 | A | C | 787.32 | N |
| 85X2-014 | 15-50 | 125.6 | -46.7 | 3.1 | A | B | 788.34 | N |
| 85X2-122 | 15-50 | 158.9 | -50.9 | 3.3 | A | B- | 789.42 | N |
| 85X3-062 | 20-40 | 309.0 | -34.8 | 3.6 | A | B- | 790.32 | N |
| 85X3-084 | 30-70 | 343.8 | -69.4 | 1.3 | A | B | 790.54 | Y |
| 85X4-089 | 25-80 | 242.1 | -57.0 | 1.7 | A | B | 792.09 | Y |
| 84X4-113 | 25-80 | 242.2 | -56.5 | 1.7 | A | B | 792.33 | Y |
| 85X5-010 | 20-70 | 97.3 | -60.0 | 2.1 | A | B | 792.80 | Y |
| 85X5-111 | 15-50 | 241.2 | -63.6 | 0.8 | A | B+ | 793.81 | Y |
| 85X6-050 | 15-50 | 90.1 | -62.8 | 1.3 | A | A- | 794.70 | Y |
| 85X6-122 | 15-80 | 152.8 | -56.2 | 1.1 | UA | A | 795.42 | Y |
| 85X7-031 | 10-80 | 141.9 | -56.3 | 1.1 | UA | A+ | 796.01 | Y |
| 86X1-120 | 15-40 | 257.1 | -27.3 | 2.7 | A | B+ | 797.60 | Y |
| 86X2-030 | 15-80 | 165.7 | -56.7 | 0.9 | UA | A+ | 798.20 | Y |
| 86X2-079 | 15-80 | 277.9 | -66.1 | 0.8 | UA | A+ | 798.69 | Y |
| 86X3-013 | 15-80 | 144.7 | -56.7 | 1.1 | UA | A | 799.53 | Y |
| 86X3-081 | 15-80 | 135.8 | -61.0 | 2.0 | UA | A | 800.21 | Y |
| 86X4-054 | 15-80 | 57.3 | -56.9 | 0.6 | UA | A | 801.44 | Y |
| 86X4-135 | 10-40 | 253.7 | 66.6 | 1.6 | A | B | 802.25 | Y |
| 86X5-030 | 20-80 | 4.3 | 55.7 | 0.5 | UA | A- | 802.70 | Y |
| 86X5-128 | 20-70 | 156.7 | 55.7 | 2.2 | A | B | 803.68 | Y |
| 86X6-051 | | ICA | | | | F | 804.41 | N |
| 86X6-077 | 20-70 | 104.5 | 65.8 | 1.2 | A | B+ | 804.67 | Y |
| 86X7-043 | 20-80 | 66.3 | 68.4 | 0.7 | UA | B+ | 805.83 | Y |
| 87X1-025 | 25-50 | 233.4 | 50.4 | 2.9 | A | B | 806.35 | Y |
| 87X1-144 | 15-80 | 114.0 | 9.1 | 2.8 | A | B- | 807.54 | N |
| 87X2-022 | 20-70 | 267.4 | 49.6 | 4.5 | A | B | 807.82 | Y |
| 87X2-124 | 25-60 | 352.6 | -60.2 | 4.4 | A | B | 808.84 | Y |
| 87X3-010 | 20-70 | 117.2 | -24.8 | 1.7 | A | B- | 809.20 | N |
| 87X3-079 | 20-70 | -48.0 | 51.1 | 2.8 | A | B | 809.89 | Y |
| 87X4-017 | 25-60 | 27.3 | 59.6 | 4.5 | A | B | 810.77 | Y |
| 87X4-140 | 25-60 | 268.9 | 53.8 | 6.7 | A | B | 812.00 | Y |
| 87X5-028 | 20-50 | 120.7 | 19.1 | 7.5 | A | C | 812.38 | N |
| 87X5-136 | 15-60 | -16.4 | 39.6 | 5.6 | A | C | 813.46 | N |
| 87X6-008 | 25-50 | 278.8 | 40.0 | 4.6 | A | B | 813.68 | Y |
| 87X6-039 | 25-80 | 183.5 | 50.3 | 3.0 | A | B | 813.99 | Y |

*Abbreviations*: Demag. Levels= demagnetization steps used for PCA calculations; ICA= Inconsistent directions; A/UA= Anchored/Unanchored fit of PCA to (0,0); MAD= Maximum Angular Deviation of PCA; Consistency of data= consistency of directions with PCA solution inclinations (range: A=excellent to F=poor).

Table A3. Hysteresis analysis data for selected samples from Holes 884B and 869A.

| Hole | Sample | Mr/Ms | Hcr/Hc | Mass (mg) |
|---|---|---|---|---|
| 869A | 5H1-027 | 0.390 | 2.001 | 56 |
| 884B | 70X1-121 | 0.227 | 2.109 | 26 |
| 884B | 70X2-040 | 0.208 | 2.344 | 44 |
| 884B | 70X6-041 | 0.214 | 2.381 | 10 |
| 884B | 71X1-139 | 0.234 | 2.33 | 14 |
| 884B | 72X1-015 | 0.212 | 2.361 | 36 |
| 884B | 72X7-051 | 0.191 | 2.673 | 15 |
| 884B | 73X1-084 | 0.220 | 2.284 | 50 |
| 884B | 73X3-068 | 0.221 | 2.281 | 35 |
| 884B | 74X3-138 | 0.232 | 2.336 | 14 |
| 884B | 75X1-096 | 0.256 | 2.265 | 50 |
| 884B | 75X3-083 | 0.196 | 2.489 | 37 |
| 884B | 76X4-110 | 0.125 | 3.241 | 30 |
| 884B | 77X4-122 | 0.261 | 2.225 | 24 |
| 884B | 78X5-066 | 0.210 | 2.508 | 48 |
| 884B | 79X5-120 | 0.216 | 2.183 | 45 |
| 884B | 80X5-120 | 0.203 | 2.619 | 9 |
| 884B | 81X4-083 | 0.328 | N/A | 23 |
| 884B | 83X2-015 | 0.404 | 1.737 | 41 |
| 884B | 86X2-030 | 0.170 | 2.276 | 55 |
| 884B | 86X4-056 | 0.170 | 2.238 | 50 |

*Abbreviations*: Mr = remanent magnetization, Ms = saturation magnetization, Hc = bulk coercivity, Hcr = coercivity of remanence.

Table A4. Leg 145 Hole 884B magnetic susceptibility (AMS) data.

| Sample | Magnetic Susceptibility ( $10E^{-6}$ SI) | | | Anisotropy Factors | | | | | | | Anisotropy | Inclination | tan(Inc) | Susceptibilty |
|---|---|---|---|---|---|---|---|---|---|---|---|---|---|---|
| | K(max) | K(int) | K(min) | L | F | P | 1/P | P` | T | q | | (°) | | ellipsoid |
| 70x1-147 | 631 | 626 | 620 | 1.007 | 1.014 | 1.021 | 0.979 | 1.022 | 0.359 | 0.385 | Weak | -62.1 | 1.89 | oblate |
| 70x3-144 | 749 | 740 | 725 | 1.002 | 1.032 | 1.034 | 0.967 | 1.038 | 0.900 | 0.052 | Weak | 51.5 | 1.26 | oblate |
| 71x4-072 | 473 | 471 | 466 | 1.002 | 1.016 | 1.018 | 0.982 | 1.02 | 0.815 | 0.098 | Weak | 49.5 | 1.17 | oblate |
| 72x2-100 | 701 | 696 | 692 | 1.002 | 1.017 | 1.019 | 0.981 | 1.021 | 0.759 | 0.129 | Weak | -57.6 | 1.58 | oblate |
| 73x3-014 | 730 | 726 | 722 | 1.006 | 1.007 | 1.014 | 0.986 | 1.014 | 0.044 | 0.631 | Weak | -41.4 | 0.88 | oblate |
| 73x5-012 | 319 | 317 | 315 | 1.002 | 1.014 | 1.016 | 0.984 | 1.017 | 0.808 | 0.102 | Weak | -50.1 | 1.20 | oblate |
| 74x1-105 | 1113 | 1108 | 1104 | 1.006 | 1.003 | 1.008 | 0.992 | 1.008 | -0.349 | 1.020 | Weak | UA | | prolate |
| 75x1-115 | 1543 | 1539 | 1535 | 1.002 | 1.004 | 1.006 | 0.994 | 1.006 | 0.422 | 0.339 | Weak | 64.3 | 2.08 | oblate |
| 76x1-041 | 1001 | 984 | 971 | 1.022 | 1.008 | 1.030 | 0.971 | 1.031 | -0.467 | 1.166 | Weak | 55.0 | 1.43 | prolate |
| 77x6-023 | 1826 | 1800 | 1769 | 1.002 | 1.043 | 1.046 | 0.956 | 1.052 | 0.894 | 0.055 | Weak | 36.4 | 0.74 | oblate |
| 78x4-143 | 3118 | 3084 | 3036 | 1.009 | 1.023 | 1.031 | 0.970 | 1.032 | 0.449 | 0.324 | Weak | -23.6 | 0.44 | oblate |
| 79x5-082 | 2518 | 2466 | 2366 | 1.002 | 1.078 | 1.080 | 0.926 | 1.092 | 0.947 | 0.028 | Moderate | UA | | oblate |
| 81x2-081 | 1203 | 1184 | 1149 | 1.008 | 1.048 | 1.056 | 0.947 | 1.061 | 0.717 | 0.156 | Weak/Mod | 59.5 | 1.70 | oblate |
| 83x5-091 | 1381 | 1374 | 1360 | 1.003 | 1.016 | 1.019 | 0.981 | 1.021 | 0.675 | 0.178 | Weak | -43.0 | 0.93 | oblate |
| 85x4-089 | 1626 | 1603 | 1563 | 1.002 | 1.045 | 1.047 | 0.955 | 1.053 | 0.913 | 0.046 | Weak | -57.0 | 1.54 | oblate |
| 85x7-031 | 1211 | 1202 | 1188 | 1.003 | 1.019 | 1.022 | 0.978 | 1.024 | 0.695 | 0.167 | Weak | -56.3 | 1.50 | oblate |
| 86x5-030 | 2142 | 2111 | 2058 | 1.001 | 1.044 | 1.044 | 0.958 | 1.051 | 0.972 | 0.014 | Weak | 55.7 | 1.47 | oblate |
| 86x7-043 | 2256 | 2234 | 2190 | 1.004 | 1.035 | 1.040 | 0.962 | 1.044 | 0.776 | 0.121 | Weak | 68.4 | 2.53 | oblate |
| 87x2-124 | 1512 | 1492 | 1460 | 1.005 | 1.032 | 1.038 | 0.963 | 1.041 | 0.728 | 0.149 | Weak | -60.2 | 1.75 | oblate |
| 87x6-039 | 1404 | 1383 | 1344 | 1.004 | 1.040 | 1.045 | 0.957 | 1.05 | 0.804 | 0.105 | Weak | 50.3 | 1.20 | oblate |

Table A5. ARM (min) /ARM (max) analysis of selected Hole 884B samples.

| Sample | Int. (Z) (A/m) | Int. (X) (A/m) | Int. (Y) (A/m) | Average X/Y | I(Z)/I(X) | I(Z)/I(Y) | ARM (min) ARM (max) | ARM ^2 | Dev. ARM | Var. ARM | Inc. (I) (deg) | tan (I) | Dev. tan(I) | Var. tan(I) | Dev (ARM) x Dev tan (I) |
|---|---|---|---|---|---|---|---|---|---|---|---|---|---|---|---|
| 884B70X1-147 | 5.63E-04 | 6.06E-04 | 6.02E-04 | 6.04E-04 | 0.929 | 0.935 | 0.932 | 0.869 | -0.004 | 2.00E-05 | -62.1 | 1.89 | 0.56 | 0.31 | -2.49E-03 |
| 884B70X3-144 | 5.63E-04 | 6.00E-04 | 5.98E-04 | 5.99E-04 | 0.937 | 0.940 | 0.939 | 0.881 | 0.002 | 4.09E-06 | 51.5 | 1.26 | -0.07 | 0.01 | -1.50E-04 |
| 884B71X4-072 | 4.74E-04 | 4.99E-04 | 4.99E-04 | 4.99E-04 | 0.951 | 0.951 | 0.951 | 0.904 | 0.014 | 1.98E-04 | 49.5 | 1.17 | -0.16 | 0.03 | -2.26E-03 |
| 884B72X2-100 | 5.63E-04 | 6.00E-04 | 5.98E-04 | 5.99E-04 | 0.937 | 0.940 | 0.939 | 0.881 | 0.002 | 4.09E-06 | -57.6 | 1.58 | 0.24 | 0.06 | 4.94E-04 |
| 884B73X3-014 | 7.48E-04 | 7.80E-04 | 7.80E-04 | 7.80E-04 | 0.960 | 0.960 | 0.960 | 0.921 | 0.023 | 5.32E-04 | -41.4 | 0.88 | -0.45 | 0.20 | -1.04E-02 |
| 884B73X5-012 | 3.47E-04 | 3.62E-04 | 3.58E-04 | 3.60E-04 | 0.960 | 0.969 | 0.964 | 0.930 | 0.028 | 7.58E-04 | -50.1 | 1.20 | -0.14 | 0.02 | -3.73E-03 |
| 884B75X1-115 | 6.40E-04 | 6.49E-04 | 6.51E-04 | 6.50E-04 | 0.987 | 0.984 | 0.985 | 0.971 | 0.048 | 2.34E-03 | 64.3 | 2.08 | 0.75 | 0.56 | 3.61E-02 |
| 884B76X1-041 | 5.94E-04 | 5.96E-04 | 6.18E-04 | 6.07E-04 | 0.996 | 0.960 | 0.978 | 0.956 | 0.041 | 1.68E-03 | 55.0 | 1.43 | 0.10 | 0.01 | 3.96E-03 |
| 884B77X6-023 | 1.38E-03 | 1.56E-03 | 1.55E-03 | 1.55E-03 | 0.887 | 0.894 | 0.891 | 0.794 | -0.046 | 2.11E-03 | 36.4 | 0.74 | -0.59 | 0.35 | 2.73E-02 |
| 884B78X4-143 | 1.53E-03 | 1.61E-03 | 1.59E-03 | 1.60E-03 | 0.952 | 0.966 | 0.959 | 0.919 | 0.022 | 4.75E-04 | -23.6 | 0.44 | -0.89 | 0.80 | -1.95E-02 |
| 884B81X2-081 | 4.02E-04 | 4.42E-04 | 4.37E-04 | 4.40E-04 | 0.908 | 0.919 | 0.914 | 0.835 | -0.023 | 5.43E-04 | 21.9 | 0.40 | -0.93 | 0.86 | 2.17E-02 |
| 884B83X5-091 | 3.99E-04 | 4.19E-04 | 4.22E-04 | 4.21E-04 | 0.951 | 0.945 | 0.948 | 0.898 | 0.011 | 1.18E-04 | -43.0 | 0.93 | -0.40 | 0.16 | -4.34E-03 |
| 884B85X4-089 | 4.16E-04 | 4.42E-04 | 4.42E-04 | 4.42E-04 | 0.942 | 0.941 | 0.942 | 0.887 | 0.005 | 2.23E-05 | -57.0 | 1.54 | 0.21 | 0.04 | 9.84E-04 |
| 884B85X7-031 | 2.57E-04 | 2.74E-04 | 2.78E-04 | 2.76E-04 | 0.937 | 0.922 | 0.929 | 0.864 | -0.008 | 5.63E-05 | -56.3 | 1.50 | 0.17 | 0.03 | -1.26E-03 |
| 884B86X5-030 | 4.55E-04 | 5.01E-04 | 4.98E-04 | 5.00E-04 | 0.906 | 0.913 | 0.910 | 0.828 | -0.027 | 7.31E-04 | 55.7 | 1.47 | 0.13 | 0.02 | -3.64E-03 |
| 884B86X7-043 | 6.09E-04 | 6.56E-04 | 6.53E-04 | 6.55E-04 | 0.928 | 0.933 | 0.930 | 0.866 | -0.006 | 4.02E-05 | 68.4 | 2.53 | 1.19 | 1.43 | -7.58E-03 |
| 884B87X2-124 | 4.43E-04 | 4.81E-04 | 4.86E-04 | 4.84E-04 | 0.921 | 0.912 | 0.916 | 0.839 | -0.021 | 4.24E-04 | -60.2 | 1.75 | 0.41 | 0.17 | -8.54E-03 |
| 884B87X6-039 | 5.61E-04 | 6.33E-04 | 6.47E-04 | 6.40E-04 | 0.886 | 0.867 | 0.877 | 0.768 | -0.060 | 3.63E-03 | 50.3 | 1.20 | -0.13 | 0.02 | 7.65E-03 |

| | |
|---|---|
| Std dev. Tan I= | 0.546 |
| mean tan I= | 1.331 |
| sum tan I= | 23.966 |
| sum ARM (min/max)= | 16.863 |
| sum (ARM min/max)^2= | 15.811 |
| mean ARM min/max= | 0.937 |
| SS(xx)= | 1.37E-02 |
| SS (yy)= | 5.07 |
| SS (xy)= | 3.44E-02 |
| R = | 0.130 |
| mean I= | 50.24 |
| Std dev. I= | 12.82 |

Table A6. Principle component analysis inclinations for Leg 145 Hole 883B discrete sediment samples.

| | Sample 145-883B- | Inclination (deg) | Depth (mbsf) | Used in colatitude |
|---|---|---|---|---|
| *Late Eocene* | 76X-1-18 | -47.6 | 720.28 | Y |
| | 76X-1-25 | -50.3 | 720.35 | Y |
| | 76X-1-65 | 15.1 | 720.75 | N |
| | 76X-1-86 | -27.8 | 720.96 | Y |
| | 76X-2-84 | -80.6 | 722.44 | N |
| | 76X-5-77 | -86.5 | 726.87 | N |
| | 76X-5-102 | -59.3 | 727.12 | Y |
| | 77X-1-24 | -72.2 | 730.14 | Y |
| | 77X-1-143 | -47.8 | 731.33 | Y |
| | 77X-2-75 | -69.1 | 732.15 | Y |
| | 77X-3-2 | -47.1 | 732.92 | Y |
| | 77X-3-70 | -46.9 | 733.60 | Y |
| | 77X-3-144 | -55.8 | 734.34 | Y |
| | 77X-4-70 | -63.7 | 735.10 | Y |
| | 77X-4-83 | -52.0 | 735.23 | Y |
| | 77X-4-102 | -63.9 | 735.42 | Y |
| | 78X-1-20 | -60.8 | 739.90 | Y |
| | 78X-1-73 | -52.8 | 740.43 | Y |
| | 78X-1-137 | -62.2 | 741.07 | Y |
| | 78X-2-8 | -60.8 | 741.28 | Y |
| | 78X-2-19 | -62.9 | 741.39 | Y |
| | 78X-2-24 | -56.2 | 741.44 | Y |
| | 78X-2-78 | -51.0 | 741.98 | Y |
| | 78X-3-108 | -49.7 | 743.78 | Y |
| | 78X-4-18 | 58.9 | 744.38 | Y |
| | 78X-4-76 | 54.6 | 744.96 | Y |
| | 78X-5-128 | 51.4 | 746.98 | Y |
| | 78X-6-18 | 47.6 | 747.38 | Y |
| | 78X-6-105 | 50.5 | 748.25 | Y |
| | 78X-6-129 | 50.1 | 748.49 | Y |
| | 79X-1-11 | 39.3 | 749.61 | Y |
| | 79X-1-31 | 16.6 | 749.81 | N |
| | 79X-2-141 | 46.9 | 752.41 | Y |
| *Early Eocene* | 83X-2-6 | -54.7 | 790.76 | Y |
| | 83X-2-71 | -53.1 | 791.41 | Y |
| | 83X-3-65 | -49.8 | 792.85 | Y |
| | 83X-3-78 | -59.6 | 792.98 | Y |
| | 83X-3-131 | -47.0 | 793.51 | Y |
| | 83X-4-26 | 31.6 | 793.96 | Y |
| | 84X-1-55 | 49.6 | 799.75 | Y |
| | 84X-CC-3 | 43.6 | 808.90 | Y |
| | 85X-1-27 | -54.8 | 809.17 | Y |
| | 85X-3-37 | 40.0 | 812.27 | Y |
| | 85X-3-58 | 28.1 | 812.48 | Y |
| | 85X-CC-41 | 37.9 | 818.90 | Y |

Table A7. Principle Component Analysis inclinations for Leg 145 Hole 887D basalt samples.

| | Sample 145-887D- | Igneous Unit | Inclination (deg) | Depth (mbsf) | Used in colatitude |
|---|---|---|---|---|---|
| | 4R-1-55 | 1 | 66.4 | 287.25 | N |
| | 4R-3-22 | 1 | 71.5 | 289.92 | N |
| | 4R-3-88 | 1 | 66.2 | 290.58 | N |
| | 4R-4-17 | 1 | 60.5 | 291.37 | N |
| | 4R-4-35 | 1 | 55.7 | 291.55 | N |
| | 5R-1-102 | 1 | 63.4 | 292.92 | N |
| | 5R-2-22 | 1 | 65.1 | 293.62 | N |
| *Group 1* | 6R-1-113 | 2 | 42.8 | 297.53 | Y |
| | 6R-1-137 | 2 | 41.7 | 297.77 | Y |
| | 7R-1-10 | 2 | 41.5 | 305.90 | Y |
| | 7R-1-143 | 2 | 40.5 | 307.23 | Y |
| | 7R-2-7 | 2 | 40.9 | 307.37 | Y |
| | 7R-2-115 | 2 | 40.0 | 308.45 | Y |
| | 7R-3-33 | 2 | 40.9 | 309.13 | Y |
| | 7R-3-123 | 2 | 40.6 | 310.03 | Y |
| | 7R-4-37 | 3 | 33.8 | 310.67 | Y |
| | 7R-4-99 | 3 | 31.9 | 311.19 | Y |
| | 8R-1-24 | 3 | 29.6 | 315.54 | Y |
| | 8R-1-90 | 3 | 25.8 | 316.20 | Y |
| | 8R-2-41 | 3 | 32.9 | 317.21 | Y |
| | 8R-2-107 | 3 | 37.4 | 317.87 | Y |
| | 8R-3-2 | 3 | 33.4 | 318.32 | Y |
| | 8R-3-56 | 3 | 29.3 | 318.86 | Y |
| *Group 2* | 10R-1-21 | 4 | -48.7 | 334.71 | Y |
| | 10R-1-36 | 4 | -48.9 | 334.86 | Y |
| | 10R-1-123 | 5 | -53.8 | 335.73 | Y |
| | 10R-1-131 | 5 | -55.5 | 335.81 | Y |
| | 10R-2-27 | 5 | -53.8 | 336.27 | Y |
| | 10R-2-101 | 5 | -56.1 | 337.01 | Y |
| | 10R-2-117 | 5 | -56.5 | 337.17 | Y |

Table A8. Principal component analysis from Site 1224 discrete samples with characteristic remanent magnetization directions that could be resolved.

| | | | | Principal Component Analysis | | | | | | | | | Unit ID | | |
|---|---|---|---|---|---|---|---|---|---|---|---|---|---|---|---|
| Sample ID (Hole-Core-Section) | Interval (cm) | Depth (mbsf) | Demag Type | Inclination (°) | Declination (°) | MAD (°) | Length (A/m) | Deviation Angle (°) | Number of Steps | Lowest Step (mT or °C) | Highest Step (mT or °C) | Option | SV Unit | Flow Unit | Strat Unit |
| **Hole 1224A** | | | | | | | | | | | | | | | |
| 1224A-05X-1 | 17 | 30.87 | AF | 3.1 | 43.8 | 1.08 | 3.97E+01 | 1.11 | 18 | 26 | 60 | FRE | 1 | 1 | I |
| 1224A-06N-1 | 11 | 32.11 | AF | 4.3 | 259.4 | 1.25 | 7.87E+00 | 3.16 | 8 | 26 | 58 | FRE | 1 | 1 | I |
| **Hole 1224D** | | | | | | | | | | | | | | | |
| 1224D-01R-1 | 46 | 25.96 | AF | -4.9 | 130.4 | 1.46 | 1.09E+01 | 10.52 | 12 | 20 | 70 | FRE | 1 | 1 | I |
| 1224D-01R-2 | 87 | 27.51 | AF | -6.4 | 8.1 | 1.04 | 5.46E+01 | 2.01 | 19 | 20 | 70 | FRE | 1 | 1 | I |
| 1224D-01R-3 | 48 | 28.58 | AF | -12.8 | 335.9 | 1.53 | 4.77E+00 | 22.76 | 4 | 22 | 70 | FRE | 1 | 1 | I |
| 1224D-01R-4 | 57 | 29.56 | AF | -4.3 | 114.0 | 1.45 | 8.65E+00 | 6.63 | 13 | 22 | 70 | FRE | 1 | 1 | I |
| 1224D-02R-1 | 15 | 35.25 | AF | -10.0 | 240.5 | 0.74 | 1.63E+02 | 1.04 | 19 | 20 | 70 | FRE | 1 | 1 | I |
| 1224D-02R-2 | 99 | 37.38 | AF | -1.6 | 107.7 | 1.38 | 5.81E+00 | 0.79 | 8 | 20 | 70 | FRE | 1 | 1 | I |
| 1224D-02R-3 | 69 | 38.40 | AF | 1.2 | 20.0 | 1.36 | 1.63E+00 | 6.89 | 4 | 20 | 55 | FRE | 1 | 1 | I |
| 1224D-02R-4 | 105 | 40.08 | AF | 3.4 | 103.3 | 0.36 | 2.93E+00 | 8.53 | 4 | 24 | 46 | FRE | 1 | 1 | I |
| 1224D-03R-1 | 26 | 44.96 | AF | 8.4 | 252.1 | 1.41 | 7.93E+00 | 57.82 | 5 | 20 | 50 | FRE | 1 | 1 | I |
| 1224D-03R-1 | 50 | 45.20 | TH | 0.2 | 246.6 | 1.21 | 1.42E+01 | 2.43 | 4 | 430 | 600 | FRE | 1 | 1 | I |
| 1224D-03R-1 | 51 | 45.21 | AF | 0.2 | 254.6 | 1.40 | 1.22E+01 | 38.82 | 6 | 22 | 65 | FRE | 1 | 1 | I |
| 1224D-03R-2 | 0 | 45.70 | TH | -3.7 | 6.4 | 1.23 | 2.07E+01 | 1.44 | 6 | 380 | 600 | FRE | 1 | 1 | I |
| 1224D-03R-2 | 81 | 46.51 | AF | 10.7 | 277.8 | 1.27 | 1.42E+00 | 48.05 | 4 | 22 | 55 | FRE | 1 | 1 | I |
| 1224D-03R-3 | 43 | 47.57 | AF | -3.3 | 35.9 | 0.93 | 9.94E+00 | 2.83 | 19 | 20 | 70 | FRE | 1 | 1 | I |
| 1224D-04R-1 | 79 | 50.09 | AF | -1.1 | 230.0 | 0.47 | 9.86E+01 | 1.46 | 18 | 22 | 70 | FRE | 1 | 2 | I |
| 1224D-04R-2 | 54 | 51.16 | TH | -11.2 | 25.9 | 3.17 | 3.13E+00 | 5.25 | 4 | 500 | 600 | FRE | 1 | 2 | I |
| 1224D-05R-1 | 64 | 51.94 | AF | 1.2 | 162.1 | 1.33 | 2.97E+01 | 5.53 | 19 | 20 | 70 | FRE | 1 | 2 | I |
| **Hole 1224E** | | | | | | | | | | | | | | | |
| 1224E-03R-1 | 84 | 27.94 | AF | -7.3 | 103.5 | 2.21 | 6.89E+00 | 50.78 | 4 | 20 | 50 | FRE | 1 | 1 | I |
| 1224E-03R-1 | 84 | 27.94 | TH | -3.6 | 100.6 | 1.23 | 2.99E+01 | 3.63 | 7 | 350 | 600 | FRE | 1 | 1 | I |
| 1224E-03R-1 | 98 | 28.08 | AF | 4.0 | 108.3 | 1.63 | 4.34E+00 | 28.73 | 4 | 20 | 42 | FRE | 1 | 1 | I |
| 1224E-03R-2 | 10 | 28.49 | TH | -1.5 | 340.6 | 2.71 | 8.59E+00 | 2.94 | 4 | 380 | 600 | FRE | 1 | 1 | I |
| 1224E-03R-2 | 48 | 28.87 | AF | -6.6 | 70.1 | 1.52 | 8.64E+00 | 38.43 | 4 | 20 | 45 | FRE | 1 | 1 | I |
| 1224E-03R-2 | 48 | 28.87 | TH | -1.8 | 71.6 | 1.07 | 1.37E+01 | 3.31 | 6 | 350 | 600 | FRE | 1 | 1 | I |
| 1224E-03R-2 | 50 | 28.89 | AF | 2.0 | 74.7 | 1.34 | 8.60E+00 | 15.42 | 6 | 20 | 44 | FRE | 1 | 1 | I |
| 1224E-03R-2 | 117 | 29.56 | AF | -3.0 | 193.1 | 0.86 | 3.83E-02 | 0.75 | 8 | 20 | 55 | FRE | 1 | 1 | I |
| 1224E-03R-2 | 117 | 29.56 | TH | -4.0 | 178.5 | 1.85 | 2.23E+01 | 1.64 | 4 | 380 | 580 | FRE | 1 | 1 | I |
| 1224E-03R-3 | 17 | 29.80 | AF | 2.5 | 286.1 | 1.28 | 2.66E+01 | 16.41 | 6 | 20 | 50 | FRE | 1 | 1 | I |
| 1224E-03R-3 | 17 | 29.80 | TH | 7.1 | 280.9 | 1.25 | 3.58E+01 | 1.17 | 6 | 440 | 600 | FRE | 1 | 1 | I |
| 1224E-03R-3 | 19 | 29.82 | AF | 4.0 | 286.0 | 0.98 | 2.48E+01 | 5.41 | 13 | 20 | 44 | FRE | 1 | 1 | I |
| 1224E-03R-3 | 65 | 30.28 | AF | -3.1 | 305.0 | 1.21 | 6.23E-02 | 0.26 | 9 | 20 | 60 | FRE | 1 | 1 | I |
| 1224E-03R-3 | 65 | 30.28 | TH | 0.2 | 309.0 | 1.30 | 1.32E+02 | 0.92 | 9 | 380 | 600 | FRE | 1 | 1 | I |
| 1224E-03R-3 | 100 | 30.63 | TH | 8.6 | 268.9 | 1.23 | 6.46E+01 | 0.96 | 6 | 430 | 600 | FRE | 1 | 1 | I |
| 1224E-03R-4 | 12 | 30.78 | AF | -0.5 | 216.4 | 1.17 | 2.71E-02 | 1.64 | 9 | 20 | 60 | FRE | 1 | 1 | I |
| 1224E-03R-4 | 12 | 30.78 | TH | 6.2 | 208.4 | 1.43 | 1.08E+02 | 0.82 | 6 | 380 | 580 | FRE | 1 | 1 | I |
| 1224E-03R-4 | 80 | 31.46 | AF | 10.5 | 357.6 | 1.12 | 7.85E+00 | 15.32 | 9 | 20 | 44 | FRE | 1 | 1 | I |
| 1224E-03R-4 | 88 | 31.54 | AF | 5.4 | 355.9 | 1.02 | 1.23E+01 | 14.5 | 4 | 20 | 45 | FRE | 1 | 1 | I |
| 1224E-03R-4 | 88 | 31.54 | TH | 12.1 | 353.4 | 1.41 | 7.28E+01 | 0.12 | 8 | 350 | 600 | FRE | 1 | 1 | I |
| 1224E-03R-4 | 109 | 31.75 | AF | 13.8 | 348.2 | 1.24 | 5.96E-03 | 2.56 | 4 | 20 | 40 | FRE | 1 | 1 | I |
| 1224E-03R-4 | 109 | 31.75 | TH | 12.6 | 354.5 | 1.06 | 8.88E+01 | 0.91 | 5 | 380 | 580 | FRE | 1 | 1 | I |
| **Hole 1224F** | | | | | | | | | | | | | | | |
| 1224F-01R-1 | 90 | 28.60 | AF | 1.5 | 146.3 | 1.57 | 3.91E-03 | 14.29 | 4 | 30 | 60 | FRE | 1 | 1 | I |
| 1224F-01R-1 | 108 | 28.78 | AF | 0.3 | 141.4 | 1.30 | 6.02E+00 | 7.13 | 10 | 20 | 48 | FRE | 1 | 1 | I |
| 1224F-01R-2 | 34 | 29.48 | AF | -5.4 | 62.4 | 1.36 | 3.45E-02 | 1.42 | 7 | 20 | 70 | FRE | 1 | 1 | I |
| 1224F-01R-2 | 69 | 29.83 | AF | 4.5 | 347.6 | 1.08 | 5.93E+00 | 10.25 | 4 | 20 | 46 | FRE | 1 | 1 | I |
| 1224F-01R-2 | 96 | 30.10 | AF | 6.6 | 149.9 | 1.43 | 5.15E-03 | 3.24 | 5 | 20 | 55 | FRE | 1 | 1 | I |
| 1224F-01R-2 | 130 | 30.44 | AF | 10.6 | 156.5 | 0.90 | 8.63E-03 | 1.89 | 4 | 20 | 55 | FRE | 1 | 1 | I |
| 1224F-01R-2 | 130 | 30.44 | TH | 8.2 | 151.8 | 1.44 | 2.83E+01 | 1.96 | 4 | 430 | 580 | FRE | 1 | 1 | I |
| 1224F-01R-3 | 21 | 30.79 | AF | 6.4 | 186.9 | 1.30 | 1.73E-02 | 2.95 | 10 | 20 | 70 | FRE | 1 | 1 | I |
| 1224F-01R-3 | 21 | 30.79 | TH | 7.3 | 180.6 | 0.83 | 5.06E+01 | 3.13 | 4 | 430 | 580 | FRE | 1 | 1 | I |
| 1224F-01R-3 | 74 | 31.32 | AF | 4.7 | 0.3 | 1.43 | 9.93E+00 | 4.43 | 10 | 20 | 48 | FRE | 1 | 1 | I |
| 1224F-01R-3 | 135 | 31.93 | TH | 7.0 | 188.3 | 1.09 | 1.18E+02 | 0.08 | 9 | 350 | 600 | FRE | 1 | 1 | I |
| 1224F-01R-3 | 137 | 31.95 | AF | 4.4 | 202.0 | 1.29 | 1.28E-02 | 2.03 | 8 | 20 | 70 | FRE | 1 | 1 | I |
| 1224F-01R-3 | 137 | 31.95 | TH | 7.7 | 202.8 | 0.86 | 7.58E+01 | 2.83 | 4 | 380 | 580 | FRE | 1 | 1 | I |
| 1224F-01R-4 | 6 | 32.15 | AF | 1.8 | 20.5 | 1.21 | 7.18E-03 | 3.84 | 5 | 20 | 70 | FRE | 1 | 1 | I |
| 1224F-01R-4 | 6 | 32.15 | TH | 8.6 | 19.7 | 1.42 | 5.74E+01 | 2.16 | 5 | 380 | 580 | FRE | 1 | 1 | I |
| 1224F-01R-4 | 33 | 32.42 | AF | 4.1 | 24.6 | 1.42 | 6.44E+00 | 3.39 | 12 | 20 | 50 | FRE | 1 | 1 | I |
| 1224F-01R-4 | 122 | 33.31 | AF | -1.8 | 337.1 | 1.20 | 9.58E-03 | 1.12 | 7 | 20 | 65 | FRE | 1 | 1 | I |
| 1224F-01R-5 | 19 | 33.71 | AF | 7.2 | 341.9 | 2.44 | 3.23E+00 | 17.02 | 8 | 20 | 48 | FRE | 1 | 1 | I |
| 1224F-02R-1 | 91 | 40.61 | AF | -0.2 | 308.9 | 1.49 | 4.96E+00 | 18.75 | 14 | 20 | 50 | FRE | 1 | 1 | I |
| 1224F-02R-1 | 93 | 40.63 | AF | 2.3 | 295.1 | 2.47 | 3.17E-03 | 110.11 | 4 | 30 | 50 | FRE | 1 | 1 | I |
| 1224F-02R-1 | 93 | 40.63 | TH | -1.8 | 303.1 | 2.46 | 4.30E+00 | 0 | 4 | 330 | 540 | ANC | 1 | 1 | I |
| 1224F-02R-2 | 14 | 41.34 | AF | 9.0 | 280.9 | 1.48 | 3.53E+00 | 88.51 | 8 | 20 | 36 | FRE | 1 | 1 | I |
| 1224F-02R-3 | 7 | 42.69 | TH | -3.2 | 291.4 | 2.23 | 7.15E+00 | 5.16 | 4 | 350 | 580 | FRE | 1 | 1 | I |
| 1224F-02R-3 | 9 | 42.71 | AF | -1.8 | 287.7 | 1.38 | 3.12E+01 | 19.5 | 14 | 20 | 50 | FRE | 1 | 1 | I |
| 1224F-02R-3 | 30 | 42.92 | AF | 1.5 | 78.2 | 1.00 | 4.79E-02 | 2.85 | 11 | 20 | 70 | FRE | 1 | 1 | I |
| 1224F-02R-3 | 59 | 43.21 | AF | -3.4 | 353.6 | 1.39 | 2.22E-02 | 1.77 | 10 | 20 | 70 | FRE | 1 | 1 | I |
| 1224F-02R-3 | 59 | 43.21 | TH | -0.5 | 354.0 | 1.88 | 1.48E+01 | 2.43 | 4 | 500 | 600 | FRE | 1 | 1 | I |
| 1224F-02R-4 | 17 | 43.93 | AF | -6.8 | 198.3 | 1.18 | 6.55E-03 | 2.33 | 5 | 20 | 60 | FRE | 1 | 1 | I |
| 1224F-02R-4 | 17 | 43.93 | TH | -7.2 | 195.9 | 0.80 | 9.87E+00 | 4.18 | 4 | 400 | 560 | FRE | 1 | 1 | I |
| 1224F-02R-4 | 20 | 43.96 | AF | -5.8 | 205.2 | 1.03 | 2.83E+00 | 10.38 | 5 | 24 | 44 | FRE | 1 | 1 | I |
| 1224F-02R-4 | 58 | 44.34 | AF | -10.5 | 203.8 | 1.38 | 5.90E-03 | 11.71 | 5 | 20 | 65 | FRE | 1 | 1 | I |
| 1224F-02R-4 | 97 | 44.73 | AF | -1.1 | 200.0 | 0.94 | 5.66E-03 | 2.93 | 5 | 20 | 70 | FRE | 1 | 1 | I |
| 1224F-02R-4 | 97 | 44.73 | TH | 1.5 | 205.6 | 1.63 | 1.34E+01 | 2.83 | 4 | 430 | 600 | FRE | 1 | 1 | I |
| 1224F-02R-4 | 140 | 45.16 | AF | 1.7 | 210.6 | 1.16 | 4.85E+00 | 23.56 | 5 | 22 | 48 | FRE | 1 | 1 | I |
| 1224F-02R-5 | 30 | 45.51 | AF | -2.5 | 162.5 | 2.40 | 3.79E-03 | 21.88 | 4 | 25 | 70 | FRE | 1 | 1 | I |
| 1224F-02R-5 | 30 | 45.51 | TH | 0.8 | 138.1 | 3.80 | 9.74E+00 | 8.68 | 4 | 400 | 600 | FRE | 1 | 1 | I |

| | | | | | | | | | | | | | | | |
|---|---|---|---|---|---|---|---|---|---|---|---|---|---|---|---|
| 1224F-02R-5 | 33 | 45.54 | AF | 4.5 | 150.3 | 1.24 | 3.36E+00 | 19.49 | 6 | 20 | 50 | FRE | 1 | 1 | I |
| 1224F-03R-2 | 22 | 49.02 | AF | -7.9 | 65.5 | 1.36 | 3.15E+00 | 4.86 | 11 | 20 | 50 | FRE | 1 | 1 | I |
| 1224F-03R-2 | 103 | 49.83 | AF | 4.1 | 162.2 | 1.20 | 4.01E-03 | 1.83 | 6 | 20 | 50 | FRE | 1 | 1 | I |
| 1224F-03R-2 | 103 | 49.83 | TH | -0.1 | 168.0 | 1.54 | 4.27E+00 | 2.98 | 4 | 380 | 600 | FRE | 1 | 1 | I |
| 1224F-03R-3 | 56 | 50.59 | AF | 2.7 | 329.0 | 1.28 | 3.23E-03 | 15.64 | 4 | 20 | 60 | FRE | 1 | 1 | I |
| 1224F-03R-3 | 56 | 50.59 | TH | -6.4 | 293.7 | 8.58 | 3.10E-01 | 25.23 | 4 | 380 | 600 | FRE | 1 | 1 | I |
| 1224F-03R-4 | 29 | 51.82 | TH | -36.2 | 71.1 | 3.03 | 2.06E+00 | 37.57 | 4 | 470 | 540 | FRE | 2 | 2* | I |
| 1224F-03R-4 | 37 | 51.90 | AF | -23.6 | 75.0 | 1.38 | 1.06E+01 | 28.58 | 12 | 20 | 50 | FRE | 2 | 2* | I |
| 1224F-04R-1 | 18 | 56.58 | AF | -32.1 | 292.5 | 2.40 | 2.86E-03 | 26.78 | 4 | 20 | 60 | FRE | 2 | 2* | I |
| 1224F-04R-1 | 18 | 56.58 | TH | -27.4 | 317.3 | 2.90 | 3.73E+00 | 2.7 | 4 | 350 | 580 | FRE | 2 | 2* | I |
| 1224F-04R-1 | 84 | 57.24 | AF | -20.1 | 7.3 | 1.11 | 6.40E-03 | 6.46 | 4 | 20 | 45 | FRE | 2 | 2* | I |
| 1224F-04R-2 | 27 | 57.57 | AF | -30.2 | 292.6 | 1.94 | 3.73E-03 | 9.03 | 4 | 20 | 60 | FRE | 2 | 2* | I |
| 1224F-04R-2 | 27 | 57.57 | TH | -28.8 | 288.0 | 4.52 | 3.45E+00 | 2.05 | 4 | 350 | 580 | FRE | 2 | 2* | I |
| 1224F-04R-2 | 30 | 57.60 | AF | -22.5 | 299.0 | 1.76 | 2.62E+00 | 18.71 | 4 | 20 | 46 | FRE | 2 | 2* | I |
| 1224F-04R-2 | 126 | 58.56 | AF | -19.3 | 82.6 | 1.66 | 2.66E-03 | 2.8 | 4 | 20 | 60 | FRE | 2 | 2* | I |
| 1224F-04R-2 | 126 | 58.56 | TH | -11.6 | 87.5 | 11.55 | 1.88E+00 | 0 | 4 | 80 | 330 | ANC | 2 | 2* | I |
| 1224F-04R-3 | 6 | 58.86 | AF | -26.9 | 89.8 | 5.37 | 1.76E-03 | 16.33 | 4 | 20 | 55 | FRE | 2 | 2* | I |
| 1224F-04R-4 | 4 | 60.27 | AF | -35.4 | 285.0 | 3.97 | 4.19E-03 | 27.69 | 4 | 20 | 55 | FRE | 2 | 2* | I |
| 1224F-04R-4 | 4 | 60.27 | TH | -27.4 | 257.5 | 2.46 | 1.14E+01 | 3.39 | 5 | 400 | 600 | FRE | 2 | 2* | I |
| 1224F-04R-5 | 30 | 61.31 | AF | -12.0 | 285.4 | 3.32 | 3.11E-03 | 18.6 | 4 | 20 | 65 | FRE | 2 | 2* | I |
| 1224F-04R-5 | 30 | 61.31 | TH | -19.8 | 284.2 | 4.73 | 4.31E+00 | 7.52 | 4 | 350 | 580 | FRE | 2 | 2* | I |
| 1224F-04R-6 | 4 | 62.52 | AF | -12.9 | 29.2 | 1.90 | 5.61E-03 | 17.36 | 4 | 20 | 70 | FRE | 2 | 2* | I |
| 1224F-05R-1 | 37 | 66.27 | AF | -32.5 | 60.2 | 1.20 | 1.03E-03 | 8.94 | 5 | 20 | 70 | FRE | 2 | 2 | II |
| 1224F-06R-1 | 102 | 76.02 | AF | 1.6 | 58.6 | 7.90 | 3.72E-01 | 11.6 | 5 | 55 | 80 | FRE | 3 | 3 | II |
| 1224F-06R-1 | 120 | 76.20 | TH | -0.2 | 119.0 | 8.30 | 3.59E+00 | 4.74 | 4 | 350 | 520 | FRE | 3 | 3 | II |
| 1224F-07R-1 | 53 | 85.03 | AF | 8.9 | 97.1 | 4.81 | 2.60E-03 | 11.11 | 4 | 20 | 50 | FRE | 3 | 3 | II |
| 1224F-08R-1 | 76 | 94.26 | TH | -2.2 | 175.4 | 5.52 | 1.42E+00 | 2.32 | 4 | 350 | 560 | FRE | 3 | 5 | II |
| 1224F-11R-1 | 80 | 121.90 | TH | -18.2 | 15.0 | 0.94 | 1.20E+01 | 0.6 | 4 | 430 | 580 | FRE | NA | 10 | II |
| 1224F-12R-1 | 16 | 128.66 | TH | -25.1 | 182.5 | 9.47 | 1.23E+00 | 23.64 | 4 | 380 | 500 | FRE | 4 | 12 | II |
| 1224F-12R-1 | 30 | 128.80 | TH | -28.8 | 321.4 | 7.84 | 1.76E+00 | 19.56 | 4 | 380 | 520 | FRE | 4 | 12 | II |
| 1224F-13R-1 | 45 | 133.95 | TH | -31.1 | 66.7 | 7.58 | 3.11E+00 | 19.34 | 4 | 380 | 560 | FRE | 4 | 13 | III |
| 1224F-13R-1 | 51 | 134.01 | TH | -25.1 | 94.4 | 7.80 | 4.97E-01 | 11.45 | 4 | 500 | 600 | FRE | 4 | 13 | III |
| 1224F-13R-1 | 51 | 134.01 | TH | -27.1 | 91.2 | 8.95 | 6.60E-01 | 11.54 | 4 | 470 | 600 | FRE | 4 | 13 | III |
| 1224F-13R-1 | 89 | 134.39 | AF | -25.1 | 32.3 | 1.27 | 1.15E-02 | 16.18 | 7 | 20 | 50 | FRE | 4 | 13 | III |
| 1224F-13R-1 | 89 | 134.39 | TH | -34.6 | 28.5 | 1.00 | 1.81E+01 | 1.25 | 6 | 380 | 600 | FRE | 4 | 13 | III |
| 1224F-13R-2 | 25 | 135.23 | AF | 0.6 | 153.8 | 1.23 | 3.27E+00 | 4.38 | 7 | 28 | 50 | FRE | NA | 13b | III |
| 1224F-13R-2 | 52 | 135.50 | AF | 3.3 | 228.8 | 1.58 | 5.72E-03 | 112.95 | 4 | 20 | 40 | FRE | NA | 13b | III |
| 1224F-13R-2 | 110 | 136.08 | AF | -21.6 | 237.1 | 1.19 | 1.03E-02 | 3.44 | 7 | 20 | 60 | FRE | 5 | 13 | III |
| 1224F-13R-2 | 110 | 136.08 | TH | -17.5 | 239.2 | 2.69 | 6.32E+00 | 6.84 | 4 | 280 | 500 | FRE | 5 | 13 | III |
| 1224F-13R-2 | 143 | 136.41 | AF | -14.8 | 97.7 | 2.81 | 3.09E-03 | 11.91 | 4 | 20 | 35 | FRE | 5 | 13 | III |
| 1224F-13R-2 | 143 | 136.41 | TH | -15.8 | 85.4 | 0.80 | 7.73E+00 | 12.76 | 4 | 330 | 540 | FRE | 5 | 13 | III |
| 1224F-14R-1 | 10 | 143.30 | TH | -18.1 | 311.4 | 0.72 | 7.59E+00 | 4.92 | 4 | 330 | 580 | FRE | 5 | 13 | III |
| 1224F-14R-1 | 48 | 143.68 | AF | -24.4 | 171.1 | 1.36 | 6.80E+00 | 10.35 | 16 | 20 | 50 | FRE | 5 | 13 | III |
| 1224F-14R-1 | 107 | 144.27 | AF | -9.2 | 83.1 | 1.31 | 3.74E+00 | 11.48 | 5 | 22 | 48 | FRE | 5 | 13 | III |
| 1224F-14R-2 | 21 | 144.83 | AF | -26.1 | 45.1 | 2.04 | 1.12E-02 | 10.08 | 4 | 20 | 35 | FRE | 5 | 13 | III |
| 1224F-14R-2 | 33 | 144.95 | TH | -25.5 | 51.1 | 0.94 | 5.03E+01 | 5.21 | 7 | 280 | 540 | FRE | 5 | 13 | III |
| 1224F-15R-1 | 57 | 152.97 | TH | -14.2 | 89.0 | 1.62 | 1.39E+01 | 9.61 | 4 | 470 | 560 | FRE | 5 | 14 | III |
| 1224F-15R-1 | 85 | 153.25 | AF | -14.7 | 17.4 | 4.18 | 1.87E-03 | 4.54 | 4 | 20 | 45 | FRE | 5 | 14 | III |
| 1224F-15R-1 | 85 | 153.25 | TH | -21.5 | 4.7 | 0.83 | 1.28E+01 | 4.47 | 4 | 470 | 580 | FRE | 5 | 14 | III |
| 1224F-15R-1 | 101 | 153.41 | AF | -11.9 | 15.2 | 1.41 | 4.77E+00 | 7.11 | 6 | 20 | 50 | FRE | 5 | 14 | III |
| 1224F-15R-1 | 127 | 153.67 | AF | -9.5 | 16.3 | 0.94 | 6.58E-03 | 7.77 | 4 | 20 | 45 | FRE | 5 | 14 | III |
| 1224F-15R-1 | 127 | 153.67 | TH | -20.6 | 23.3 | 1.33 | 2.14E+01 | 2.49 | 4 | 470 | 580 | FRE | 5 | 14 | III |

Demag Type: AF = alternating field demagnetization; TH = themal demagnetization.
The mean paleomagnetic direction is estimated from the demagnetization data using the principal component analysis (PCA) method of Kirschvink (1980).

The best-fit line that passes through the vector demagnetization data is not forced to be anchored to the origin of vector demagnetization space, but is allowed to freely fit the data.
To avoid data possibly contaminated by the drilling overprint, we do not use demagnetization steps <20 mT or <280°C. We use an iterative search program to find
and delete demagnetization steps in any interval that give directions that are outliers relative to directions from other demagnetization steps from that interval.
PCA parameters, in addition to the direction (inclination and declination), are:

MAD = Maximum angular deviation.
Length = Distance from origin of the vector demagnetization space to the centroid of the data used to find the best-fit line.
Deviation Angle = The angle between the best-fit line and a line that passes through the origin and centroid.
Number of Steps = Number of demagnetization steps used in finding the best-fit line.
Lowest Step = The lowest demagnetization step used in finding the best-fit line.
Highest Step = The highest demagnetization step used in finding the best-fit line.

SV Unit: Secular variation units are those units with inclinations distinct from stratigraphic adjacent (overlying and underlying) units. We only considered a unit distinct when more than 4 samples were obtained. Thus, the NA (not applicable) are for intervals where too few samples giving distinct inclinations were available to define a separte SV unit.

Cooling Unit: These are from Table T5 from the Site 1224 Chapter (Stephen et al., 2003). The 2* denotes that these intervals were listed as the being in the uppermost basalt unit (Cooling Unit 1 in Table T5), which was an error in that table. They really belong to Cooling Unit 2. The cooling units are based mainly on where contacts were observed in recovered cores. The true number of cooling units will be somewhat larger than the 14 units noted.

Strat Unit: These are the three stratigraphic units the basalt section was divided into by (Shipboard Scientific Party, 2003). The divisions were based primarily on flow morphology.

Table A9. Mean colatitudes for Site 1224.

| | | McFadden-Reid Method* | | | | | | | Cox-Gordon Method** | | |
|---|---|---|---|---|---|---|---|---|---|---|---|
| SV Unit | Number of Observations | Observed Inclination (°) | Unbiased Inclination (°) | 1-d 95% Confidence (°) | Precision Parameter | Observed Colatitude (°) | Unbiased Colatitude (°) | 1-d 95% Confidence (°) | Unbiased Colatitude (°) | Std. Error (°) | 1-d 95% Confidence (°) |
| 1 | 83 | 1.01 | 1.01 | 1.5 | 95.6 | 90.5 | 90.5 | 0.7 | 90.5 | 0.3 | 0.7 |
| 2 | 17 | -24.63 | -24.87 | 4.7 | 53.6 | 77.1 | 77.0 | 2.7 | 76.9 | 1.1 | 2.8 |
| 3 | 4 | 2.02 | 2.03 | 10.1 | 140.3 | 91.0 | 91.0 | 5.1 | 91.0 | 1.2 | 5.1 |
| 4 | 7 | -28.13 | -28.18 | 4.1 | 247.1 | 75.0 | 75.0 | 2.5 | 75.0 | 0.8 | 2.9 |
| 5 | 15 | -17.69 | -17.77 | 3.6 | 109.3 | 80.9 | 80.9 | 1.9 | 80.9 | 0.8 | 1.9 |
| Mean | 5 | -13.6 | -13.9 | 22.7 | 16.2 | 83.1 | 82.9 | 12.3 | 82.8 | 4.2 | 8.2 |

Inclinations are from basalts extruded during reversed polarity Chron 20R.

* = calculations using the method of McFadden and Reid (1982).

** = calculations using the method of Cox and Gordon (1984).

Table A10. Paleomagnetic pole mean age calculations.

| Oligocene | Site | Colatitude | Average age (Ma) | Importance (I) | age*I | Std. dev. |
|---|---|---|---|---|---|---|
| | S68-24 | 105.6 | 32.7 | 0.18 | 5.9 | 1.8 |
| | K72-39 | 91.7 | 30.6 | 0.35 | 10.7 | 0.4 |
| | K78020 | 87.9 | 26.1 | 0.15 | 3.9 | 1.8 |
| | K78523 | 88.0 | 30.9 | 0.15 | 4.6 | 0.3 |
| | K78023 | 90.9 | 26.4 | 0.15 | 4.0 | 1.5 |
| | ODP 1218 | 87.5 | 26.3 | 0.25 | 6.6 | 2.6 |
| | ODP 1218 | 87.4 | 29.2 | 0.13 | 3.8 | 0.0 |
| | ODP 1219 | 92.9 | 32.0 | 0.15 | 4.8 | 0.9 |
| | ODP 884B | 48.8 | 30.0 | 0.03 | 0.9 | 0.0 |
| | ODP 869A | 85.4 | 32.5 | 0.20 | 6.5 | 1.8 |
| | Midway Reef | 71.3 | 27.7 | 0.07 | 1.9 | 0.2 |
| | Midway Sand Is. | 75.7 | 27.7 | 0.03 | 0.8 | 0.1 |
| | 887D avg | 62.3 | 27.4 | 0.02 | 0.5 | 0.1 |
| | Site 597 | 119.5 | 27.5 | 0.09 | 2.5 | 0.4 |
| | Site 63 | 94.0 | 32.4 | 0.05 | 1.6 | 0.4 |
| average age 29.5 | | | | 2 | 29.5 | 2.5 |

| Late Eocene | Site | Colatitude | Average age (Ma) | Importance (I) | age*I | Std. dev. |
|---|---|---|---|---|---|---|
| | ODP 883B | 53.9 | 41.8 | 0.05 | 2.1 | 0.3 |
| | ODP 884B | 64.5 | 41.2 | 0.11 | 4.5 | 0.4 |
| | ODP 1220 | 94.5 | 42.2 | 0.43 | 18.1 | 3.9 |
| | S68-24 | 100.6 | 36.3 | 0.31 | 11.3 | 2.6 |
| | M7039 | 106.6 | 37.0 | 0.46 | 17.0 | 2.2 |
| | Abbott | 83.9 | 41.5 | 0.15 | 6.2 | 0.8 |
| | Stanley | 95.3 | 39.3 | 0.17 | 6.7 | 0.0 |
| | Colahan | 84.8 | 38.5 | 0.17 | 6.5 | 0.1 |
| | Willoughby | 90.7 | 39.3 | 0.15 | 5.9 | 0.0 |
| average age 39.2 | | | | 2 | 39.2 | 2.3 |

| Early Eocene | Site | Colatitude | Average age (Ma) | Importance (I) | age*I | Std. dev. |
|---|---|---|---|---|---|---|
| | ODP 1206 | 68.5 | 49.1 | 0.13 | 6.4 | 0.0 |
| | ODP 883B | 61.5 | 52.5 | 0.04 | 2.1 | 0.6 |
| | ODP 884B | 49.7 | 45.7 | 0.04 | 1.8 | 0.3 |
| | DSDP 430A | 69.9 | 55.2 | 0.06 | 3.3 | 2.6 |
| | DSDP 577A | 74.7 | 55.8 | 0.11 | 6.1 | 5.6 |
| | DSDP 577A | 74.5 | 51.3 | 0.12 | 6.2 | 0.8 |
| | DSDP 577 | 76.4 | 54.7 | 0.15 | 8.2 | 5.5 |
| | DSDP 577 | 74.0 | 50.6 | 0.18 | 9.1 | 0.7 |
| | ODP 1220 | 92.4 | 44.1 | 0.50 | 22.1 | 10.2 |
| | ODP 1224 | 82.8 | 46.2 | 0.06 | 2.8 | 0.3 |
| | K78-0-12 | 93.1 | 47.5 | 0.35 | 16.6 | 0.4 |
| | Daikakuji -East | 93.4 | 46.7 | 0.09 | 4.2 | 0.3 |
| | Daikakuji -West | 71.8 | 46.7 | 0.09 | 4.2 | 0.3 |
| | Annei | 107.6 | 52.0 | 0.08 | 4.2 | 0.9 |
| average age 48.6 | | | | 2 | 48.6 | 3.8 |

Table A10. Continued.

| Paleocene | Site | Colatitude | Average age (Ma) | Importance (I) | age*I | Std. dev. |
|---|---|---|---|---|---|---|
| with MMA skewness | DSDP 199 | 95.9 | 62.0 | 0.04 | 2.5 | 0.0 |
| | DSDP 585 | 90.3 | 61.6 | 0.04 | 2.5 | 0.0 |
| | DSDP 577 | 75.8 | 57.7 | 0.03 | 1.7 | 0.6 |
| | DSDP 577 | 76.0 | 60.9 | 0.04 | 2.4 | 0.1 |
| | DSDP 577 | 78.6 | 64.1 | 0.04 | 2.6 | 0.2 |
| | DSDP 577 | 77.5 | 65.5 | 0.04 | 2.6 | 0.5 |
| | DSDP 577A | 73.0 | 60.1 | 0.03 | 1.8 | 0.1 |
| | DSDP 577A | 75.9 | 63.1 | 0.02 | 1.3 | 0.0 |
| | DSDP 577A | 77.2 | 65.2 | 0.04 | 2.6 | 0.4 |
| | DSDP 433C | 63.2 | 61.3 | 0.05 | 3.1 | 0.0 |
| | DSDP 432A | 57.7 | 56.2 | 0.02 | 1.1 | 0.7 |
| | ODP 1205 | 64.0 | 55.6 | 0.03 | 1.7 | 1.3 |
| | Paumakua | 102.6 | 65.5 | 0.01 | 0.7 | 0.1 |
| | Kautu | 86.9 | 58.4 | 0.02 | 1.2 | 0.3 |
| | MMA 25r | 78.2/4.8 | 57.0 | 0.37 | 21.1 | 9.7 |
| | MMA27r-29 | 73.1/7.7 | 64.0 | 1.18 | 75.5 | 4.1 |
| average age 62.1 | | | | 2 | 62.1 | 3.0 |

| Paleocene | Site | Colatitude | Average age (Ma) | Importance (I) | age*I | Std. dev. |
|---|---|---|---|---|---|---|
| no MMA skewness | DSDP 199 | 95.9 | 62.0 | 0.1 | 6.2 | 0.1 |
| | DSDP 585 | 90.3 | 61.6 | 0.1 | 6.2 | 0.0 |
| | DSDP 577 | 75.8 | 57.7 | 0.08 | 4.6 | 0.9 |
| | DSDP 577 | 76.0 | 60.9 | 0.09 | 5.5 | 0.0 |
| | DSDP 577 | 78.6 | 64.1 | 0.1 | 6.4 | 0.9 |
| | DSDP 577 | 77.5 | 65.5 | 0.1 | 6.6 | 2.0 |
| | DSDP 577A | 73.0 | 60.1 | 0.07 | 4.2 | 0.1 |
| | DSDP 577A | 75.9 | 63.1 | 0.05 | 3.2 | 0.2 |
| | DSDP 577A | 77.2 | 65.2 | 0.09 | 5.9 | 1.5 |
| | DSDP 433C | 63.2 | 61.3 | 0.25 | 15.3 | 0.0 |
| | DSDP 432A | 57.7 | 56.2 | 0.05 | 2.8 | 1.2 |
| | ODP 1205 | 64.0 | 55.6 | 0.16 | 8.9 | 4.8 |
| | Paumakua | 102.6 | 65.5 | 0.29 | 19.0 | 5.7 |
| | Kautu | 86.9 | 58.4 | 0.47 | 27.4 | 3.3 |
| average age 61.1 | | | | 2 | 61.1 | 3.2 |

| Maastrichtian | Site | Colatitude | Average age (Ma) | Importance (I) | age*I | Std. dev. |
|---|---|---|---|---|---|---|
| with MMA skewness | GPC3 | 78.9 | 67.5 | 0.03 | 2.0 | 0.1 |
| | DSDP 577 | 78.7 | 66.8 | 0.12 | 8.0 | 1.0 |
| | DSDP 577A | 72.7 | 66.8 | 0.06 | 4.0 | 0.5 |
| | DSDP 577A | 73.1 | 68.2 | 0.03 | 2.0 | 0.1 |
| | DSDP 585-585A | 91.3 | 68 | 0.18 | 12.2 | 0.5 |
| | DSDP 315A | 98.9 | 70.35 | 0.02 | 1.4 | 0.0 |
| | ODP 871 | 98.9 | 68.3 | 0.02 | 1.4 | 0.0 |
| | Wageman | 105.7 | 71.9 | 0.02 | 1.4 | 0.1 |
| | Paumakua | 102.6 | 65.5 | 0.02 | 1.3 | 0.3 |
| | Musina | 97.2 | 69.6 | 0.02 | 1.4 | 0.0 |
| | MMA 32 (N.Far.) | 68.4/9.2 | 71.1 | 1.1 | 78.2 | 2.3 |
| | MMA 27r-31 | 73.2/4.6 | 68 | 0.38 | 25.8 | 1.0 |
| average age 69.6 | | | | 2 | 69.6 | 1.7 |

Table A10. Continued.

| Maastrichtian | Site | Colatitude | Average age (Ma) | Importance (I) | age*I | Std. dev. |
|---|---|---|---|---|---|---|
| no MMA skewness | GPC3 | 78.9 | 67.5 | 0.4 | 27.0 | 0.2 |
| | DSDP 577 | 78.7 | 66.8 | 0.28 | 18.7 | 0.6 |
| | DSDP 577A | 72.7 | 66.8 | 0.14 | 9.4 | 0.3 |
| | DSDP 577A | 73.1 | 68.2 | 0.06 | 4.1 | 0.0 |
| | DSDP 585-585A | 91.3 | 68.0 | 0.39 | 26.5 | 0.0 |
| | DSDP 315A | 98.9 | 70.4 | 0.38 | 26.7 | 1.7 |
| | ODP 871 | 98.9 | 68.3 | 0.06 | 4.1 | 0.0 |
| | Wageman | 105.7 | 71.9 | 0.08 | 5.8 | 1.1 |
| | Paumakua | 102.6 | 65.5 | 0.09 | 5.9 | 0.7 |
| | Musina | 97.2 | 69.6 | 0.12 | 8.4 | 0.2 |
| average age 68.2 | | | | 2 | 68.2 | 1.5 |

Table A11. Age calculations for time window poles.

| Pole | Site | Age (Ma) | Std. Dev. | Importance (I) | I*age |
|---|---|---|---|---|---|
| *25 Ma* | | | | | |
| | K72-39 | 30.6 | 1.49 | 0.13 | 3.97 |
| | K78020 | 26.1 | 0.27 | 0.24 | 6.26 |
| | K78523 | 30.9 | 3.35 | 0.24 | 7.42 |
| | K78023 | 26.4 | 0.16 | 0.24 | 6.32 |
| | ODP-1218 | 23.1 | 1.13 | 0.07 | 1.62 |
| | ODP-1218 | 23.3 | 1.18 | 0.08 | 1.87 |
| | ODP-1218 | 23.7 | 0.48 | 0.04 | 0.95 |
| | ODP-1218 | 24.1 | 0.67 | 0.07 | 1.68 |
| | ODP-1218 | 24.1 | 0.46 | 0.05 | 1.21 |
| | ODP-1218 | 24.4 | 0.47 | 0.06 | 1.46 |
| | ODP-1218 | 24.7 | 0.18 | 0.03 | 0.74 |
| | ODP-1218 | 25.0 | 0.33 | 0.07 | 1.75 |
| | ODP-1218 | 25.7 | 0.08 | 0.04 | 1.03 |
| | ODP-1218 | 26.4 | 0.03 | 0.06 | 1.59 |
| | ODP-1218 | 27.3 | 0.00 | 0.05 | 1.36 |
| | ODP-1218 | 28.0 | 0.04 | 0.05 | 1.40 |
| | ODP-1218 | 28.3 | 0.07 | 0.05 | 1.42 |
| | ODP-1218 | 28.5 | 0.09 | 0.05 | 1.42 |
| | ODP-1218 | 28.6 | 0.09 | 0.04 | 1.15 |
| | ODP-1218 | 29.1 | 0.07 | 0.02 | 0.58 |
| | ODP-1218 | 29.6 | 0.12 | 0.02 | 0.59 |
| | ODP-1218 | 30.0 | 0.41 | 0.05 | 1.50 |
| | ODP-884B | 30.0 | 0.39 | 0.05 | 1.50 |
| | Midway-Reef | 27.7 | 0.03 | 0.12 | 3.32 |
| | Midway-Sand | 27.7 | 0.01 | 0.05 | 1.39 |
| | 887D-avg | 27.4 | 0.00 | 0.01 | 0.27 |
| | Site-597 | 27.5 | 0.00 | 0.02 | 0.55 |
| | | | 2.41 | 2.00 | 27.16 |
| average age= | 27.2 | | | | |
| uncertainty= | 2.4 | | | | |

| Pole | Site | Age (Ma) | Std. Dev. | Importance (I) | I*age |
|---|---|---|---|---|---|
| *30 Ma* | | | | | |
| | s68-24 | 32.7 | 1.86 | 0.17 | 5.56 |
| | K72-39 | 30.6 | 0.16 | 0.12 | 3.67 |
| | K78020 | 26.1 | 1.52 | 0.14 | 3.65 |
| | K78523 | 30.9 | 0.32 | 0.14 | 4.33 |
| | K78023 | 26.4 | 1.30 | 0.14 | 3.69 |
| | ODP-1218 | 25.0 | 1.74 | 0.09 | 2.25 |
| | ODP-1218 | 25.7 | 0.67 | 0.05 | 1.29 |
| | ODP-1218 | 26.4 | 0.70 | 0.08 | 2.11 |
| | ODP-1218 | 27.3 | 0.27 | 0.06 | 1.64 |
| | ODP-1218 | 28.0 | 0.12 | 0.06 | 1.68 |
| | ODP-1218 | 28.3 | 0.07 | 0.06 | 1.70 |
| | ODP-1218 | 28.5 | 0.06 | 0.07 | 1.99 |
| | ODP-1218 | 28.6 | 0.04 | 0.06 | 1.72 |
| | ODP-1218 | 29.1 | 0.00 | 0.03 | 0.87 |
| | ODP-1218 | 29.6 | 0.00 | 0.05 | 1.48 |
| | ODP-1218 | 30.0 | 0.03 | 0.07 | 2.10 |
| | ODP-1219 | 30.4 | 0.03 | 0.03 | 0.91 |
| | ODP-1219 | 30.9 | 0.09 | 0.04 | 1.24 |
| | ODP-1219 | 32.2 | 0.32 | 0.04 | 1.29 |
| | ODP-1219 | 33.6 | 0.86 | 0.05 | 1.68 |
| | ODP-1219 | 34.3 | 1.18 | 0.05 | 1.71 |
| | ODP-884B | 30.0 | 0.01 | 0.03 | 0.90 |
| | ODP 869A | 32.5 | 1.83 | 0.19 | 6.18 |
| | Midway-Reef | 27.7 | 0.20 | 0.07 | 1.94 |
| | Midway-Sand | 27.7 | 0.09 | 0.03 | 0.83 |
| | 887D-avg | 27.4 | 0.04 | 0.01 | 0.27 |
| | Site-597 | 27.5 | 0.11 | 0.03 | 0.82 |
| | Site 63 | 32.4 | 0.36 | 0.04 | 1.30 |
| | | | 2.64 | 2.00 | 29.40 |
| average age= | 29.4 | | | | |
| uncertainty= | 2.6 | | | | |

| Pole | Site | Age (Ma) | Std. Dev. | Importance (I) | I*age |
|---|---|---|---|---|---|
| *35 Ma* | | | | | |
| | s68-24 | 32.7 | 0.06 | 0.16 | 5.23 |
| | K72-39 | 30.6 | 1.67 | 0.22 | 6.72 |
| | K78523 | 30.9 | 0.75 | 0.13 | 4.02 |
| | ODP-1218 | 30.0 | 1.92 | 0.18 | 5.41 |
| | ODP-1219 | 30.4 | 0.50 | 0.06 | 1.83 |
| | ODP-1219 | 30.9 | 0.65 | 0.11 | 3.40 |
| | ODP-1219 | 32.2 | 0.11 | 0.10 | 3.22 |
| | ODP-1219 | 33.6 | 0.01 | 0.16 | 5.37 |
| | ODP-1219 | 34.3 | 0.12 | 0.13 | 4.45 |
| | ODP-884B | 30.0 | 0.22 | 0.02 | 0.60 |
| | ODP-869A | 32.5 | 0.11 | 0.17 | 5.53 |
| | Site 63 | 32.4 | 0.03 | 0.04 | 1.30 |
| | s68-24 | 36.3 | 1.35 | 0.15 | 5.45 |
| | m70-39 | 37.0 | 2.60 | 0.19 | 7.03 |
| | ODP-883B | 41.8 | 1.43 | 0.02 | 0.84 |
| | Stanley | 39.3 | 1.44 | 0.04 | 1.57 |
| | Abbott | 38.7 | 1.16 | 0.04 | 1.55 |
| | Colahan | 38.5 | 1.08 | 0.04 | 1.54 |
| | Willoughby | 39.3 | 1.44 | 0.04 | 1.57 |
| | | | 2.88 | 2.00 | 33.30 |
| average age= | 33.3 | | | | |
| uncertainty= | 2.9 | | | | |

| Pole | Site | Age (Ma) | Std. Dev. | Importance (I) | I*age |
|---|---|---|---|---|---|
| *40 Ma* | | | | | |
| | s68-24 | 36.3 | 4.39 | 0.29 | 10.53 |
| | m70-39 | 37.0 | 3.87 | 0.38 | 14.06 |
| | ODP-883B | 41.8 | 0.10 | 0.04 | 1.67 |
| | ODP-1220 | 44.1 | 6.42 | 0.42 | 18.52 |
| | ODP-1220 | 42.2 | 0.93 | 0.23 | 9.71 |
| | ODP-1224 | 46.2 | 1.81 | 0.05 | 2.31 |
| | ODP-884B | 45.7 | 1.82 | 0.06 | 2.74 |
| | ODP-884B | 41.2 | 0.08 | 0.09 | 3.70 |
| | Stanley | 39.3 | 0.09 | 0.11 | 4.32 |
| | Abbott | 38.7 | 0.24 | 0.11 | 4.26 |
| | Colahan | 38.5 | 0.31 | 0.11 | 4.24 |
| | Willoughby | 39.3 | 0.09 | 0.11 | 4.32 |
| | | | 3.17 | 2.00 | 40.19 |
| average age= | 40.2 | | | | |
| uncertainty= | 3.2 | | | | |

Table A11. Continued.

| Pole | Site | Age (Ma) | Std. Dev. | Importance (I) | I*age |
|---|---|---|---|---|---|
| *45Ma* | | | | | |
| | k78-0-12 | 47.5 | 0.50 | 0.32 | 15.20 |
| | ODP-883B | 52.5 | 1.95 | 0.05 | 2.63 |
| | ODP-883B | 41.8 | 0.81 | 0.04 | 1.67 |
| | DSDP-577 | 50.6 | 3.78 | 0.20 | 10.12 |
| | DSDP-577A | 51.3 | 3.49 | 0.14 | 7.18 |
| | ODP-1220 | 44.1 | 1.76 | 0.38 | 16.76 |
| | ODP-1220 | 42.2 | 3.29 | 0.20 | 8.44 |
| | ODP-1224 | 46.2 | 0.00 | 0.05 | 2.31 |
| | ODP 884B | 45.7 | 0.02 | 0.05 | 2.29 |
| | ODP-884B | 41.2 | 1.82 | 0.07 | 2.88 |
| | ODP-1206 | 49.1 | 1.21 | 0.15 | 7.37 |
| | Stanley | 39.3 | 3.39 | 0.07 | 2.75 |
| | Daikakuji -E | 46.7 | 0.01 | 0.07 | 3.27 |
| | Daikakuji-W | 46.7 | 0.01 | 0.07 | 3.27 |
| | Willoughby | 39.3 | 3.39 | 0.07 | 2.75 |
| | Annei | 52.0 | 2.31 | 0.07 | 3.64 |
| | | | 3.72 | 2.00 | 46.25 |
| average age= | 46.3 | | | | |
| uncertainty= | 3.7 | | | | |

| Pole | Site | Age (Ma) | Std. Dev. | Importance (I) | I*age |
|---|---|---|---|---|---|
| *50 Ma* | | | | | |
| | k78-0-12 | 47.5 | 0.30 | 0.34 | 16.15 |
| | ODP-883B | 52.5 | 0.50 | 0.03 | 1.58 |
| | ODP-883B | 41.8 | 1.34 | 0.03 | 1.25 |
| | DSDP-577 | 54.7 | 5.41 | 0.14 | 7.65 |
| | DSDP-577 | 50.6 | 0.80 | 0.17 | 8.60 |
| | DSDP-577a | 55.8 | 5.89 | 0.11 | 6.13 |
| | DSDP-577a | 51.3 | 0.95 | 0.12 | 6.15 |
| | ODP-1220 | 44.1 | 9.57 | 0.51 | 22.49 |
| | ODP-1224 | 46.2 | 0.30 | 0.06 | 2.77 |
| | ODP 884B | 45.7 | 0.30 | 0.04 | 1.83 |
| | ODP-1206 | 49.1 | 0.06 | 0.13 | 6.38 |
| | DSDP-430A | 55.2 | 2.75 | 0.06 | 3.31 |
| | Daikakuji -E | 46.7 | 0.27 | 0.09 | 4.20 |
| | Daikakuji-W | 46.7 | 0.27 | 0.09 | 4.20 |
| | Annei | 52.0 | 1.02 | 0.08 | 4.16 |
| | | | 3.85 | 2.00 | 48.43 |
| avergae age= | 48.4 | | | | |
| uncertainty= | 3.9 | | | | |

| Pole | Site | Age (Ma) | Std. Dev. | Importance (I) | I*age |
|---|---|---|---|---|---|
| *55 Ma* with MMA | | | | | |
| | ODP-883B | 52.5 | 0.48 | 0.02 | 1.05 |
| | DSDP-577 | 54.7 | 0.52 | 0.07 | 3.83 |
| | DSDP-577 | 50.6 | 2.76 | 0.06 | 3.04 |
| | DSDP-577a | 55.8 | 0.13 | 0.05 | 2.79 |
| | DSDP-577a | 51.3 | 1.50 | 0.04 | 2.05 |
| | DSDP-430A | 55.2 | 0.14 | 0.03 | 1.66 |
| | DSDP 585 | 61.6 | 1.22 | 0.07 | 4.31 |
| | DSDP 577 | 57.7 | 0.01 | 0.06 | 3.46 |
| | DSDP 577 | 60.9 | 0.87 | 0.07 | 4.26 |
| | DSDP 577A | 60.1 | 0.43 | 0.06 | 3.60 |
| | DSDP 199 | 62.0 | 1.49 | 0.07 | 4.34 |
| | DSDP 432A | 56.2 | 0.03 | 0.02 | 1.12 |
| | ODP 1205 | 55.6 | 0.19 | 0.06 | 3.34 |
| | Annei | 52.0 | 1.74 | 0.06 | 3.12 |
| | MMA 25r | 57.8 | 0.20 | 1.26 | 72.80 |
| | | | 2.42 | 2.00 | 57.38 |
| average age= | 57.4 | | | | |
| uncertainty= | 2.4 | | | | |

| Pole | Site | Age (Ma) | Std. Dev. | Importance (I) | I*age |
|---|---|---|---|---|---|
| *55 Ma* no MMA | | | | | |
| | ODP-883B | 52.5 | 0.16 | 0.03 | 1.58 |
| | DSDP-577 | 54.7 | 0.00 | 0.10 | 5.47 |
| | DSDP-577 | 50.6 | 1.61 | 0.09 | 4.55 |
| | DSDP-577a | 55.8 | 0.06 | 0.07 | 3.90 |
| | DSDP-577a | 51.3 | 0.90 | 0.07 | 3.59 |
| | DSDP-430A | 55.2 | 0.01 | 0.08 | 4.42 |
| | DSDP 585 | 61.6 | 4.97 | 0.11 | 6.77 |
| | DSDP 577 | 57.7 | 0.83 | 0.10 | 5.77 |
| | DSDP 577 | 60.9 | 4.06 | 0.11 | 6.70 |
| | DSDP 577A | 60.1 | 2.46 | 0.09 | 5.40 |
| | DSDP 199 | 62.0 | 5.15 | 0.10 | 6.20 |
| | DSDP 432A | 56.2 | 0.08 | 0.04 | 2.25 |
| | ODP 1205 | 55.6 | 0.09 | 0.15 | 8.34 |
| | Annei | 52.0 | 6.87 | 0.86 | 44.72 |
| | MMA 25r | 57.8 | 0.00 | 0.00 | 0.00 |
| | | | 3.69 | 2.00 | 54.83 |
| average age= | 54.8 | | | | |
| uncertainty= | 3.7 | | | | |

Table A11. Continued.

| Pole | Site | Age (Ma) | Std. Dev. | Importance (I) | I*age | | Std. Dev. | Importance (I) | I*age |
|---|---|---|---|---|---|---|---|---|---|
| *60 Ma* | | | | | | *60 Ma* | | | |
| with MMA | | | | | | no MMA | | | |
| | ODP-883B | 52.5 | 0.92 | 0.01 | 0.53 | | 2.22 | 0.02 | 1.05 |
| | DSDP-577 | 54.7 | 1.67 | 0.03 | 1.64 | | 4.91 | 0.07 | 3.83 |
| | DSDP-577a | 55.8 | 0.81 | 0.02 | 1.12 | | 2.65 | 0.05 | 2.79 |
| | DSDP-430A | 55.2 | 0.48 | 0.01 | 0.55 | | 2.45 | 0.04 | 2.21 |
| | DSDP 585 | 61.6 | 0.01 | 0.04 | 2.46 | | 0.22 | 0.10 | 6.16 |
| | DSDP 577 | 57.7 | 0.58 | 0.03 | 1.73 | | 2.27 | 0.08 | 4.62 |
| | DSDP 577 | 60.9 | 0.06 | 0.04 | 2.44 | | 0.41 | 0.09 | 5.48 |
| | DSDP 577 | 64.1 | 0.16 | 0.04 | 2.56 | | 0.10 | 0.09 | 5.77 |
| | DSDP 577A | 60.1 | 0.13 | 0.03 | 1.80 | | 0.62 | 0.07 | 4.20 |
| | DSDP 577A | 63.1 | 0.02 | 0.02 | 1.26 | | 0.00 | 0.04 | 2.52 |
| | DSDP 577A | 65.2 | 0.37 | 0.04 | 2.61 | | 0.41 | 0.09 | 5.86 |
| | DSDP 199 | 62.0 | 0.00 | 0.04 | 2.48 | | 0.11 | 0.10 | 6.20 |
| | DSDP-433C | 61.3 | 0.03 | 0.05 | 3.07 | | 0.45 | 0.15 | 9.20 |
| | DSDP 432A | 56.2 | 0.35 | 0.01 | 0.56 | | 0.93 | 0.02 | 1.12 |
| | ODP 1205 | 55.6 | 1.27 | 0.03 | 1.67 | | 4.96 | 0.09 | 5.00 |
| | GPC 3 | 67.5 | 1.46 | 0.05 | 3.38 | | 11.40 | 0.57 | 38.48 |
| | Paumakua | 65.5 | 0.12 | 0.01 | 0.66 | | 0.80 | 0.13 | 8.52 |
| | Kautu | 65.3 | 0.10 | 0.01 | 0.65 | | 1.03 | 0.20 | 13.06 |
| | MMA25r | 57.8 | 6.74 | 0.36 | 20.80 | | 0.00 | 0.00 | 0.00 |
| | MMA 27r-29r | 63.9 | 3.82 | 1.13 | 72.25 | | 0.00 | 0.00 | 0.00 |
| | | | 3.09 | 2.00 | 62.10 | | 4.24 | 2.00 | 63.03 |
| average age= | 62.1 | | | | | 63.0 | | | |
| uncertainty= | 3.1 | | | | | 4.2 | | | |

| Pole | Site | Age (Ma) | Std. Dev. | Importance (I) | I*age | | Std. Dev. | Importance (I) | I*age |
|---|---|---|---|---|---|---|---|---|---|
| *65 Ma* | | | | | | *65 Ma* | | | |
| with MMA | | | | | | no MMA | | | |
| | DSDP 585 | 61.6 | 0.36 | 0.03 | 1.85 | | 1.37 | 0.06 | 3.69 |
| | DSDP 577 | 57.7 | 1.61 | 0.03 | 1.73 | | 4.47 | 0.06 | 3.46 |
| | DSDP 577 | 60.9 | 0.51 | 0.03 | 1.83 | | 1.77 | 0.06 | 3.65 |
| | DSDP 577 | 64.1 | 0.04 | 0.04 | 2.56 | | 0.30 | 0.06 | 3.85 |
| | DSDP 577A | 60.1 | 0.75 | 0.03 | 1.80 | | 1.97 | 0.05 | 3.00 |
| | DSDP 577A | 63.1 | 0.08 | 0.02 | 1.26 | | 0.32 | 0.03 | 1.89 |
| | DSDP 577A | 65.2 | 0.00 | 0.03 | 1.95 | | 0.08 | 0.06 | 3.91 |
| | DSDP 199 | 62.0 | 0.28 | 0.03 | 1.86 | | 1.13 | 0.06 | 3.72 |
| | DSDP-433C | 61.3 | 0.56 | 0.04 | 2.45 | | 2.53 | 0.10 | 6.13 |
| | Odp 871 | 68.3 | 0.21 | 0.02 | 1.37 | | 0.16 | 0.04 | 2.73 |
| | DSDP 577 | 66.8 | 0.25 | 0.08 | 5.34 | | 0.03 | 0.15 | 10.02 |
| | DSDP 577A | 66.8 | 0.12 | 0.04 | 2.67 | | 0.02 | 0.07 | 4.68 |
| | DSDP 577A | 68.2 | 0.20 | 0.02 | 1.36 | | 0.10 | 0.03 | 2.05 |
| | DSDP-585 | 68.0 | 0.97 | 0.11 | 7.48 | | 0.56 | 0.20 | 13.60 |
| | DSDP-315A | 70.4 | 1.13 | 0.04 | 2.81 | | 5.41 | 0.34 | 23.57 |
| | GPC 3 | 67.5 | 0.24 | 0.04 | 2.70 | | 0.47 | 0.35 | 23.29 |
| | Paumakua | 65.5 | 0.00 | 0.01 | 0.66 | | 0.05 | 0.07 | 4.59 |
| | Kautu | 65.3 | 0.00 | 0.01 | 0.65 | | 0.12 | 0.11 | 7.18 |
| | Musina | 69.6 | 0.21 | 0.01 | 0.70 | | 1.18 | 0.11 | 7.66 |
| | MMA 27r-29r | 63.9 | 1.22 | 1.01 | 64.58 | | 0.00 | 0.00 | 0.00 |
| | MMA 29r-31 | 68.0 | 2.98 | 0.33 | 22.45 | | 0.00 | 0.00 | 0.00 |
| total | | | 2.42 | 2.00 | 65.04 | | 3.32 | 2.00 | 66.33 |
| average age= | 65.0 | | | | | 66.3 | | | |
| uncertainty= | 2.4 | | | | | 3.3 | | | |

Table A11. Continued

| Pole | Site | Age (Ma) | Std. Dev. | Importance (I) | I*age | | Std. Dev. | Importance (I) | I*age |
|---|---|---|---|---|---|---|---|---|---|
| *70 Ma* | | | | | | *70 Ma* | | | |
| with MMA | | | | | | no MMA | | | |
| | DSDP-585 | 61.6 | 1.04 | 0.03 | 1.85 | | 2.36 | 0.07 | 4.31 |
| | DSDP 577 | 64.1 | 0.33 | 0.03 | 1.92 | | 0.74 | 0.07 | 4.49 |
| | DSDP 577 | 65.5 | 0.11 | 0.03 | 1.97 | | 0.28 | 0.08 | 5.24 |
| | DSDP 577A | 65.2 | 0.16 | 0.03 | 1.95 | | 0.34 | 0.07 | 4.56 |
| | DSDP 199 | 62.0 | 0.88 | 0.03 | 1.86 | | 2.01 | 0.07 | 4.34 |
| | Odp 871 | 68.3 | 0.01 | 0.01 | 0.68 | | 0.04 | 0.05 | 3.42 |
| | DSDP 577 | 66.8 | 0.03 | 0.07 | 4.68 | | 0.06 | 0.18 | 12.02 |
| | DSDP 577A | 66.8 | 0.01 | 0.03 | 2.00 | | 0.03 | 0.09 | 6.01 |
| | DSDP 577A | 68.2 | 0.01 | 0.02 | 1.36 | | 0.03 | 0.04 | 2.73 |
| | DSDP-585 | 68.0 | 0.03 | 0.10 | 6.80 | | 0.10 | 0.24 | 16.32 |
| | DSDP-315A | 70.4 | 0.17 | 0.02 | 1.41 | | 3.12 | 0.35 | 24.62 |
| | GPC 3 | 67.5 | 0.00 | 0.02 | 1.35 | | 0.01 | 0.35 | 23.63 |
| | Paumakua | 65.5 | 0.04 | 0.01 | 0.66 | | 0.24 | 0.07 | 4.59 |
| | Wageman | 71.9 | 0.20 | 0.01 | 0.72 | | 1.24 | 0.06 | 4.31 |
| | Kautu | 65.3 | 0.05 | 0.01 | 0.65 | | 0.47 | 0.11 | 7.18 |
| | Musina | 69.6 | 0.05 | 0.01 | 0.70 | | 0.50 | 0.10 | 6.96 |
| | MMA 27r-29r | 63.9 | 7.78 | 0.64 | 40.92 | | 0.00 | 0.00 | 0.00 |
| | MMA 32 | 71.1 | 9.42 | 0.70 | 49.77 | | 0.00 | 0.00 | 0.00 |
| | MMA 29r-31 | 68.0 | 0.08 | 0.20 | 13.61 | | 0.00 | 0.00 | 0.00 |
| | | | 3.19 | 2.00 | 67.43 | | 2.41 | 2.00 | 67.36 |
| average age= | 67.4 | | | | | 67.4 | | | |
| uncertainty= | 3.2 | | | | | 2.4 | | | |
| *75 Ma* | | | | | | *75 Ma* | | | |
| with MMA | | | | | | no MMA | | | |
| | DSDP-585 | 68.0 | 0.94 | 0.24 | 16.32 | | 0.72 | 0.74 | 50.32 |
| | DSDP-315A | 70.4 | 0.00 | 0.02 | 1.41 | | 0.67 | 0.36 | 25.33 |
| | GPC 3 | 67.5 | 0.18 | 0.03 | 2.03 | | 0.86 | 0.39 | 26.33 |
| | Wageman | 71.9 | 0.07 | 0.02 | 1.44 | | 1.87 | 0.22 | 15.82 |
| | Musina | 69.6 | 0.00 | 0.02 | 1.39 | | 0.11 | 0.29 | 20.18 |
| | MMA 32 | 71.1 | 1.52 | 1.23 | 87.45 | | 0.00 | 0.00 | 0.00 |
| | MMA 29r-31 | 68.0 | 1.66 | 0.44 | 29.94 | | 0.00 | 0.00 | 0.00 |
| | | | 1.48 | 2.00 | 69.98 | | 1.45 | 2.00 | 68.99 |
| average age= | 70.0 | | | | | 69.0 | | | |
| | 1.5 | | | | | 1.5 | | | |